AD703 949

UNCLASSIFIED
Security Classification

DOCUMENT CONTROL DATA - R & D

(Security classification of title, body of abstract and indexing annotation must be entered when the overall report is classified)

1. ORIGINATING ACTIVITY (Corporate author)
IIT Research Institute
10 West 35th Street
Chicago, Illinois 60616

2a. REPORT SECURITY CLASSIFICATION

2b. GROUP
N/A

3. REPORT TITLE
FRAGMENTATION HAZARD STUDY
Phase III
FRAGMENT HAZARDS FROM DETONATION OF MULTIPLE MUNITIONS IN OPEN STORES

4. DESCRIPTIVE NOTES (Type of report and inclusive dates)
Final Report (October 1969 to September 1970)

5. AUTHOR(S) (First name, middle initial, last name)
D. I. Feinstein
H. H. Nagaoka

6. REPORT DATE	7a. TOTAL NO. OF PAGES	7b. NO. OF REFS
August 1971	90	2

8a. CONTRACT OR GRANT NO.	9a. ORIGINATOR'S REPORT NUMBER(S)
DAHC-04-69-C-0056	J-6176
b. PROJECT NO.	
c.	9b. OTHER REPORT NO(S) (Any other numbers that may be assigned this report)
d.	

10. DISTRIBUTION STATEMENT
Distribution of this document is unlimited.

11. SUPPLEMENTARY NOTES	12. SPONSORING MILITARY ACTIVITY
	Armed Services Explosives Safety Bd Forrestal Building, Room GB270 Washington, D.C. 20314

13. ABSTRACT

An investigation of fragment hazards from multiple munitions in open stores is described. The objectives of the study were to estimate fragment hazards as a function of type and quantity of munitions, and configurations of the store.

To this end an analytic stack model has been developed from insight gained on a series of small- and full-scale tests. A series of tests were run utilizing M117 750-lb bombs in order to verify the analytic stack model. Another set of verification tests were run with 155mm shells.

The results of the bomb test, when compared to the results of an analytic simulation obtained from the stack model, indicate that reasonable answers are being obtained. The shell tests, however, resulted in unexpected effects. These effects indicate that while the analytic stack model has reasonable validity for bomb stacks, simulation of shell stacks will have to consider additional effects such as the variation of individual fragment size with munition case design, stack configuration and mode of initiation. The fragment weight spectrum appears to be strongly influenced by factors other than munition design for projectiles, and to differ markedly from that for the ideal single source burst.

DD FORM 1 NOV 68 1473 REPLACES DD FORM 1473, 1 JAN 64, WHICH IS OBSOLETE FOR ARMY USE.

UNCLASSIFIED
Security Classification

UNCLASSIFIED

Security Classification

14 KEY WORDS	LINK A		LINK B		LINK C	
	ROLE	WT	ROLE	WT	ROLE	WT

Security Classification

Final Technical Report IITRI J6176
Contract DAHC-04-69-C-0056

FRAGMENTATION HAZARD STUDY
Phase III
FRAGMENT HAZARDS FROM DETONATION OF MULTIPLE MUNITIONS IN OPEN STORES

Armed Services Explosives Safety Board
Forrestal Building, Room GB270
Washington, D. C. 20314

D. I. Feinstein
H. H. Nagaoka

IIT Research Institute
10 West 35th Street
Chicago, Illinois 60616

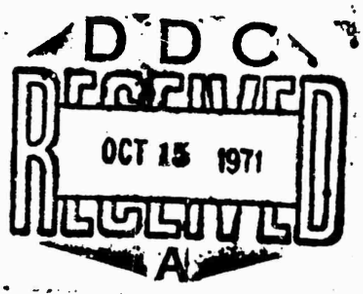

August 1971

Final Report for Period October 1969 to September 1970

FOREWORD

Under Contract DAHC-04-69-C-0056 between IIT Research Institute (IITRI) and the U.S. Army Research Office-Durham, IITRI is performing a study of fragmentation hazards from accidental detonation of munition stores. This is the final report on Phase III of the study carried out during the period October 1969 to September 1970.

The work is being conducted for the Armed Services Explosives Safety Board and supervised by Col. W. Cameron III, Chairman, Dr. T. A. Zaker, Explosives Scientist and Mr. R. G. Perkins, Safety Engineer. Principal contributors to the presently reported work include D. I. Feinstein, H. H. Nagaoka, J. D. Rouse and O. J. Stepanek, who served as project engineer. The technical work was directed and approved by L.A.C. Barbarek, Manager of Civil Engineering Systems and Explosives, H. S. Napadensky, Senior Research Engineer, and A. H. Wiedermann, Science Advisor.

Respectfully submitted,
IIT RESEARCH INSTITUTE

D. I. Feinstein,
Research Engineer

Arne H. Wiedermann,
Science Advisor

APPROVED:

L.A.C. Barbarek
Manager
Civil Engineering Systems
and Explosives

ABSTRACT

An investigation of fragment hazards from multiple munitions in open stores is described. The objectives of the study were to estimate fragment hazards as a function of type and quantity of munitions, and configurations of the store.

To this end an analytic stack model has been developed from insight gained on a series of small- and full-scale tests. A series of tests were run utilizing M117 750-lb bombs in order to verify the analytic stack model. Another set of verification tests were run with 155mm shells.

The results of the bomb test, when compared to the results of an analytic simulation obtained from the stack model, indicate that reasonable answers are being obtained. The shell tests, however, resulted in unexpected effects. These effects indicate that while the analytic stack model has reasonable validity for bomb stacks, simulation of shell stacks will have to consider additional effects such as the variation of individual fragment size with munition case design, stack configuration, and mode of initiation. The fragment weight spectrum appears to be strongly influenced by factors other than munition design for projectiles, and to differ markedly from that for the ideal single source burst.

TABLE OF CONTENTS

LIST OF ILLUSTRATIONS

LIST OF ILLUSTRATIONS (concluded)

LIST OF TABLES

FRAGMENTATION HAZARD STUDY PHASE III

1. INTRODUCTION

Existing quantity-distance standards for the manufacture, handling, and storage of munitions are based on the net weight of explosive filler contained in the devices in an unsubdivided magazine, or operating building unit. Safe distances are prescribed in tabular form essentially proportional to the cube root of the explosive weight.

Because peak blast pressures from explosions of different yield are the same at distances scaled by the cube root of the respective explosive weights, existing standards imply that the acceptable risk to a given target is based on a peak blast overpressure criterion alone. On the other hand, the field of fragments projected to the far field from accidental explosion of a munition store, consisting of inert munition component fragments and secondary fragments from any enclosure, does not satisfy the same similarity rules as does the airblast. Thus, defining an acceptable blast overpressure level at a target implies the acceptance of different levels of risk of damage by fragments, depending on the quantity and composition of the munition store and its enclosure.

To develop quantity-distance standards based on consistent blast and fragment hazard levels requires determination of the damage risk due to fragments from accidental explosions as a function of the quantity and type of munitions, and of the characteristics of the source environment and the vulnerability of the target. A previous report (Ref. 1), covered the initial two phases of a multiphase program aimed at applying engineering analysis, supplementary experimental efforts, and currently available data on fragmentation and damage criteria to the problem of estimating fragment hazards at explosives manufacturing and storage sites. While that report considered only single munitions, this report is concerned with extending the analytic techniques to include stacks of munitions.

1.1 Problem Background

A full understanding of the current research program described in this report can only be achieved in the context of the total continuing program. This overall program has the following objectives:

(1) To develop methodology for estimating risks of injury and damage from fragments

- to a wide range of human, mechanical and structural targets,
- at all ground ranges and orientations within the limit of vulnerability,
- from detonations of various types and quantities of munitions,
- in open stores and in protective enclosures,
- expressing risk on a probability basis.

(2) To apply the methodology in determining levels of risk from fragments for a series of actual real-world sites.

(3) To conduct the analytical, empirical, and experimental studies required to fill gaps in current knowledge in support of the development of the methodology.

Phase I of this study was concerned with establishing quantitative damage criteria in terms of fragment mass, velocity, and attack angle for various targets including standing personnel, vehicles, aircraft, buildings and open weapon stores. In Phase II an analytical model was developed to predict the density of fragments and the probability of damage to the targets considered in Phase I from explosion of individual munitions of various types. These included gun projectiles and general-purpose bombs. Here damage probability contours were obtained in polar coordinates for a horizontal orientation of the munition axis in each case.

1.2 Program Objectives

In Phase III, the current research activity, the intent has been to extend the fragment hazard model, developed under Phase II for individual munitions, to the case of multiple munitions in open stores. The objectives of the study were:

(1) To extend the fragment hazard model to estimate quantity-distance relationships for fragment hazards as a function of type and quantity of munitions, and configurations of the store.

(2) To conduct full-scale verification tests to validate these quantity-distance relationships.

1.3 Program Accomplishments

The major result of this study has been the demonstration that an analytic model can be developed to describe the initial fragment field of a stack of munitions. The input to the model consists of data describing the initial fragment field of a single munition in the stack and the stack configuration. Although the model's validity has only been demonstrated for fragments corresponding to the side material of bombs, the philosophy of the stack model allows for incorporating the effects due to the nose and base material. However, these incorporations depend upon empirical or analytic representation of the magnification phenomena due to ogive and boattail curvature. Another significant accomplishment has been to identify the fact that stacks of projectiles result in completely different types of fragments than single projectiles. This indicates that parameters describing other factors, such as munition case design, stack configuration, and mode of initiation, will have to be included in the stack model for thick-wall munitions.

1.4 Program Highlights

The ensuing sections of this report are organized in such a way as to present the philosophy of the stack model, the tests in support of this philosophy, the tests

to validate this philosophy, and the comparative data which demonstrate the feasibility of the model. Finally conclusions concerning the research activity and recommendations as to further effort are presented.

2. STACK MODEL PHILOSOPHY

The analytic model, developed under the previous Phase II activity, for estimating fragment hazards included these salient features:

(1) Input defining the initial spatial field of fragment masses, velocities and elevation angles,

(2) Application of trajectory analysis to determine terminal positions and terminal ballistic properties of fragments, and

(3) Utilization of vulnerability functions derived from available data for the determination of impact and damage probabilities.

In extending the analysis to include multiple munition sources (i.e., stacks) the only feature above which is affected is the input describing the initial spatial field.

This input, for the single munition, was obtained from existing test results (Ref. 2) describing the fragmentation effectiveness of various munitions. No such similar information exists for stack configurations of these munitions. Therefore, the major research task in the Phase III study has been to establish a means of transforming the input data for a single munition into the corresponding input for a stack of this same munition.

A series of small-scale experiments indicated that zones of material enhancement tend to develop within areas where one munition shades another in a stack. This pattern of material enhancement has been observed to be directly related to the stack configuration. Outside the enhancement areas the initial spatial field of a stack is seen to behave similarly to a single munition. Another phenomenon that was observed was that the amount

of fragments recovered down range (i.e., not completely blocked by other fragments) was related to that surface area of the stack which was free from shading effects.

Utilizing these results a simple stack model has been developed which relates stack configuration to appropriate adjustment of the initial spatial field input, for a single munition, in order to obtain the corresponding initial spatial field input for the stack. This model is predicated upon these rules:

(1) Only material, which is initially unshaded in the stack, is available for down range fragment production.

(2) This available material behaves like a single munition except in special regions where material enhancement takes place.

(3) Fragments from munitions in stacks are similar in appearance to fragments from corresponding single munitions.

The input data available, describing the initial spatial fragment field for a single munition, were adjusted to reflect the observed results of the small-scale stack experiments. That is, simple multiplication factors were applied to the input data for selected elevation angles to reflect the material enhancement effect which takes place in these regions as observed in the small-scale experiments.

In order to gain insight into this stack model and attempt to verify it, two full-scale 750-lb bomb tests were run to obtain final spatial field data for two distinct stack configurations. Initial spatial field input for this munition was available and so were enhancement rules for one of the stack configurations. These enhancement rules were formulated from the set of small-scale experimental results. These small-scale experiments, however, only simulated the full-scale experiments for fragments originating from the sides of the stacked munitions. Therefore, it was necessary to investigate parametrically how much polar angle was involved in the distribution of side-spray fragments.

From results which will be presented in the following sections, it is apparent that the stack model is producing final field results which are comparable to experimental results in applicable regions.

3. SMALL-SCALE TESTS

Fundamental information concerning the mechanism of fragment interaction was investigated for simultaneously detonated, clustered munitions. To implement the experimental phase of this task, a small size munition model was designed specifically to minimize the variables associated with conventional munition configurations. A ball-type, preformed-fragment explosive model was designed and demonstrated to provide a uniform ball-fragment distribution. A complementary 16-sided, closed arena facility was constructed which provided comprehensive fragment interaction data.

The program investigated 12 distinct munition cluster configurations in 20 experiments to study the initial fragment field for simultaneously detonated stacked munitions. Data reduction techniques were developed to provide both qualitative and quantitative data concerning the mechanism of fragment interaction.

It should be emphasized that the small-scale experiments were designed to examine the initial fragment field for munition side-spray. Although analogous fragment interaction behavior may be expected from stacked ogival noses and base configurations of conventional munitions, the unique metal parts configurations will result in highly complex fragment interactions. No attempt was made to simulate nose and base material interactions in the small-scale experiments.

3.1 Small-Scale Munition Design

The paucity of data concerning the mechanism of fragment interaction for stacked munitions suggested that the model munition design be physically simple in geometry and predictable in behavior. Based upon this premise, a ball-type, preformed-fragment munition configuration was designed with a simple cylindrical shape. An efficient fabrication technique was devised in which an exact number of ball bearings with uniform spacing could be assembled on the munition wall using nonmetallic components.

The design details of the small-scale munition configuration are shown on Figure 1. The munition assembly procedure may be described as follows:

- Clean 3/16 in. diameter steel balls are arranged in the hex-pack pattern on a tray.
- Double-adhesive plastic tape is cut to 2 in. by 4-15/16 in. size and aligned on the ball arrangement.
- The taped balls are transferred to the outer diameter of the fiber tube (1-1/2 in. inner diameter, 1/32 in. wall thickness, 4-1/4 in. long). Two lengths of taped balls are placed on the fiber tube in a manner that maintains the basic ball pattern.
- After the balls are checked for uniform spacing and number, the exposed balls on the fiber tube are covered with adhesive tape for ease of handling.
- The munition assembly is then filled with 190 grams of C-4 explosive.

The small-scale munition assembly incorporates these specifications.

Total Munition Weight: 505 grams
Number of Balls: 675 (3/16 in. diam 52100 steel)
Weight of Inert Nonmetals: 16 grams
Weight of C-4 Explosive: 190 grams
Explosive-to-metal Ratio: 0.635
Nominal Dimensions: 2 in. diam x 4-1/4 in. long

It was decided initially that the small-scale munition clusters would be detonated simultaneously to reduce the number of experimental variables. This was accomplished by attaching equal lengths of primacord to each munition in a given group, and initiating the clustered free ends of the primacord with a single detonator. It was determined that 175-grain primacord in conjunction with a No. 6 blasting cap initiator could be used reliably.

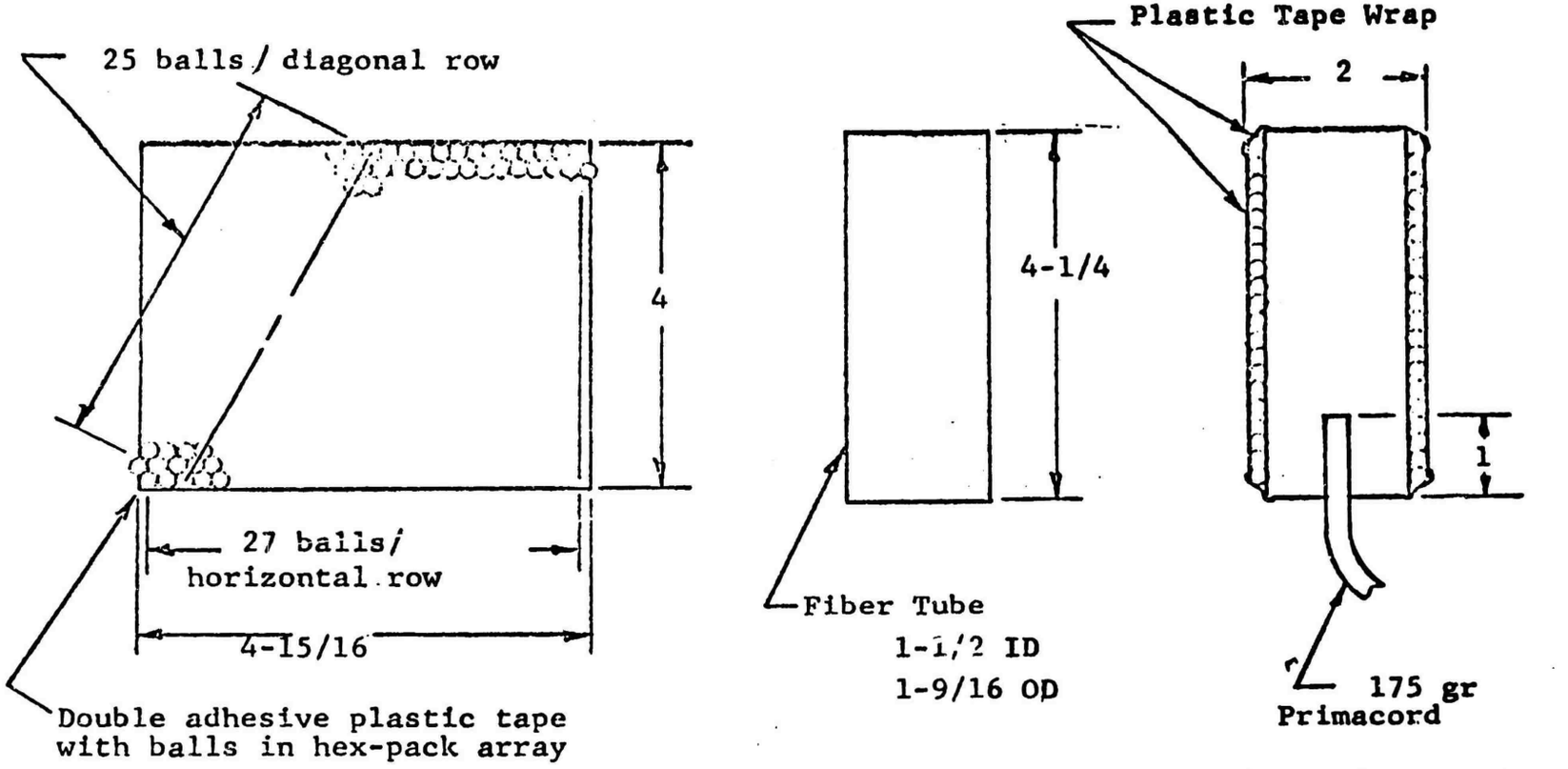

Munition Specifications	
Weight of munition	505 gm
Number of balls	675 (3-16 in. diam, 52100 steel)
Weight of balls	299 gm
Weight of C-4 explosive	190 gm
Weight of Inert Nonmetals	16 gm

Figure 1 SMALL-SCALE MUNITION SPECIFICATIONS

Experiments were conducted to compare the fragment interaction pattern between the preformed-fragment munition and a naturally fragmenting munition. The conventional munition specifications were calculated to match the ball-type munition. Applying data obtained at IITRI under Contract F08635-67-C-0056 (IITRI Project B6077) the naturally fragmenting munition was designed with these specifications:

Total Munition Weight: 509 grams
Weight of Cylinder: 319 grams
Weight of C-4 Explosive: 190 grams
Explosive-to-metal Ratio: 0.596
Cylinder Material: AISI 4130, Heat Treat R_c 28-30
Cylinder Dimensions: 1-1/2 in. inner diam,
1/8 in. wall thickness,
4 in. long

3.2 Explosive Arena Design

To obtain meaningful fragment interaction data for clustered munitions, a 16-sided closed arena facility was constructed using standard plywood panels that enclosed a diameter of about 20 ft. The arena configuration represented a balanced compromise between the performance characteristics of the small-size explosive model and a manageable arena structure which would provide full fragment interaction data.

The design details incorporated in the small-scale explosive arena facility are illustrated in Figure 2. Several design considerations were examined to implement the construction of the arena facility. Based upon a 20 ft diameter arena, calculations indicated that the small-size explosive model would yield a fragment pattern width of about 4 ft on the witness sheets. The blast pressures expected on the witness panels were calculated for various clusters of explosive models. These data suggested that the panels should be erected with minimum restraint and be permitted to blow outward under blast loading.

Thus, a 16-sided closed arena configuration with a nominal 10 ft radius was designed using standard 4 ft by 8 ft by 1/2 in. thick plywood sheets. Each 4 ft wide unit provided 22-1/2 degrees of fragment impact coverage.

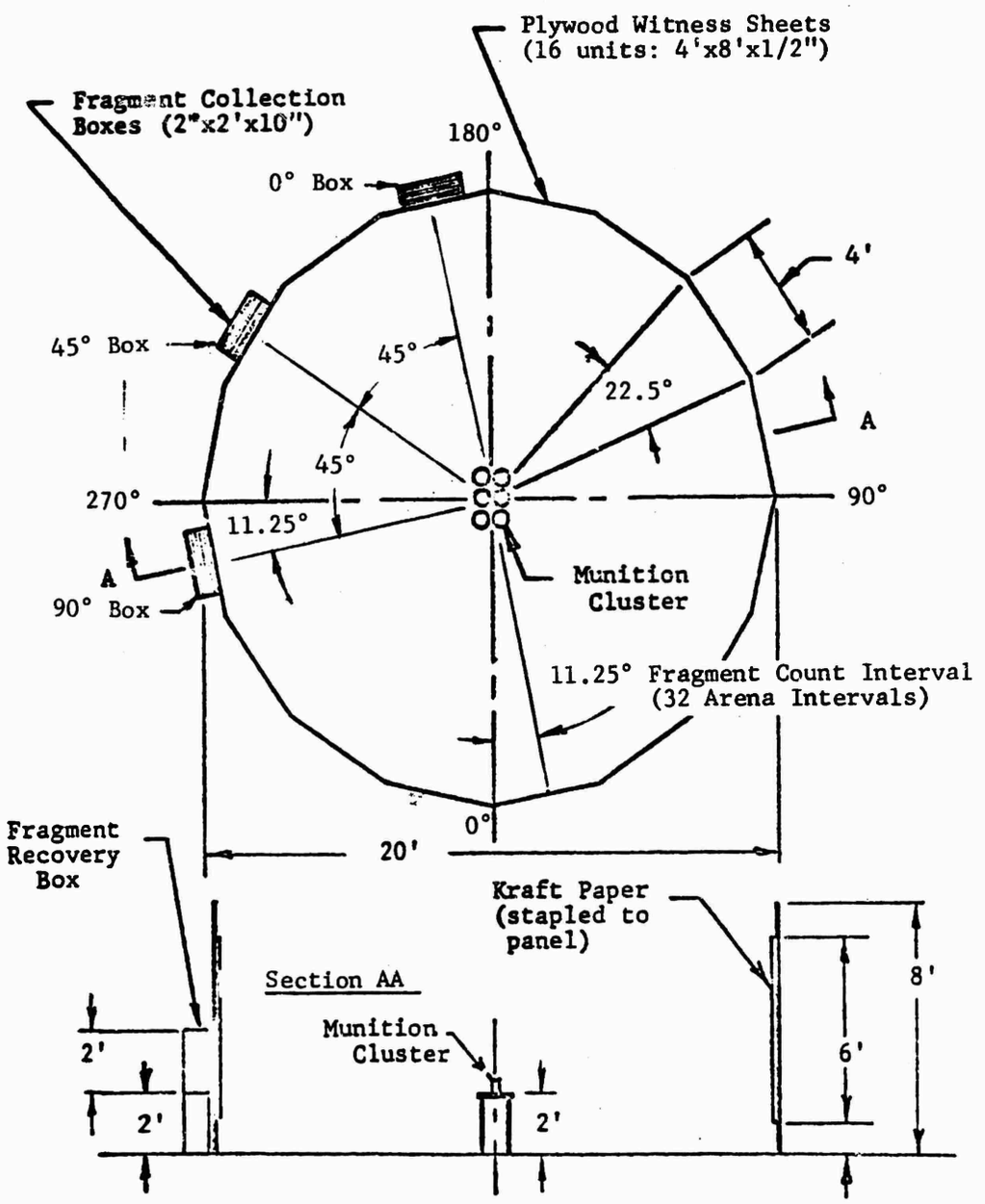

Figure 2 SMALL-SCALE MUNITION ARENA FACILITY

Utilizing these input data, the explosive arena facility was constructed as follows:

- An 8 ft high earth mound about 40 ft in diameter was prepared at the IITRI-KOP Explosive Research field laboratory near LaPorte, Indiana.
- Inside the horseshoe earth mound, steel marker stakes were driven into the ground to locate the corners of the plywood witness units.
- Boards 2 by 4 in., 5 ft long were nailed as hinges for the vertical edges of the plywood witness sheet.
- As each unit was assembled, the bottom corners of the sheets were set at the steel marker stakes.
- The last unit served as the arena doorway, to be closed after final experimental preparations were completed.
- Heavy kraft paper was stapled to each plywood sheet to obtain clean fragment impact perforations and provide a portable data record to facilitate the data reduction process.
- Each kraft witness paper was marked with identification numbers, and a cross-hair was drawn across arena markers to align the munition cluster which was placed 2 ft above ground level.

In addition, three fragment collection boxes were fabricated from 20 layers of Celotex panels, (each 2 ft by 2 ft by 1/2 in.), to record fragment penetration data and to provide physical recovery of fragment samples. Heavy kraft paper was placed at each inch of Celotex depth to obtain clean penetration data. The three collection boxes were placed 45 degrees apart immediately behind the plywood witness sheets to record penetration data for the side, end, and vertical edge of the munition clusters.

3.3 Small-Scale Munition Experimental Results

Twenty diagnostic experiments were conducted to study the initial fragment field for simultaneously detonated clustered munitions. These experiments involved 92 small-scale munitions which were clustered in 12 distinct configurations. The basic study was conducted with parameters associated with stacked M117 bombs in open store to facilitate data correlation with the full-size validation tests that are discussed in Section 4 of this report.

The initial fragment field was examined for munition cluster configurations shown in Figure 3. The one-half radius spacing (r = 1/2 radius) for clustered munitions was selected for detailed study to correspond with the normal spacing for stacked M117 munitions. In particular, configurations 6 and 8 are analogous to the munition configurations used in the full-size validation tests.

3.3.1 Small-Scale Munition Experimental Program

A tabulated summary of the configuration runs used in the small-scale munition experiments is shown on Table 1. During the early stages of the program, the experimental design structure was developed for the small-scale munition study. The first three experiments were conducted to establish performance characteristics for the single ball-type munition and the complementary explosive arena structure. The 1/4 and 3/16 in. diameter steel ball-type munitions were fabricated and detonated successfully with 175-grain primacord initiated by a No. 6 blasting cap. A count was made of the intact ball perforations on the witness sheets of the nominal 20 ft diameter arena. These data indicated that both ball-type munitions provided relatively uniform ball-fragment distribution with negligible loss to shattered balls. Since the 3/16 in. diameter steel-ball munition has an explosive charge-to-metal ratio closer to that of the M117 bomb, this unit was selected as the standard explosive model.

Experiments 4 and 5 were conducted to investigate the fragmentation characteristics for clustered ball-type munitions using the 16-sided explosive arena facility. For a given array of clustered models it was

A. <u>One-Half Radius Spacing</u> (r = 1/2 radius)

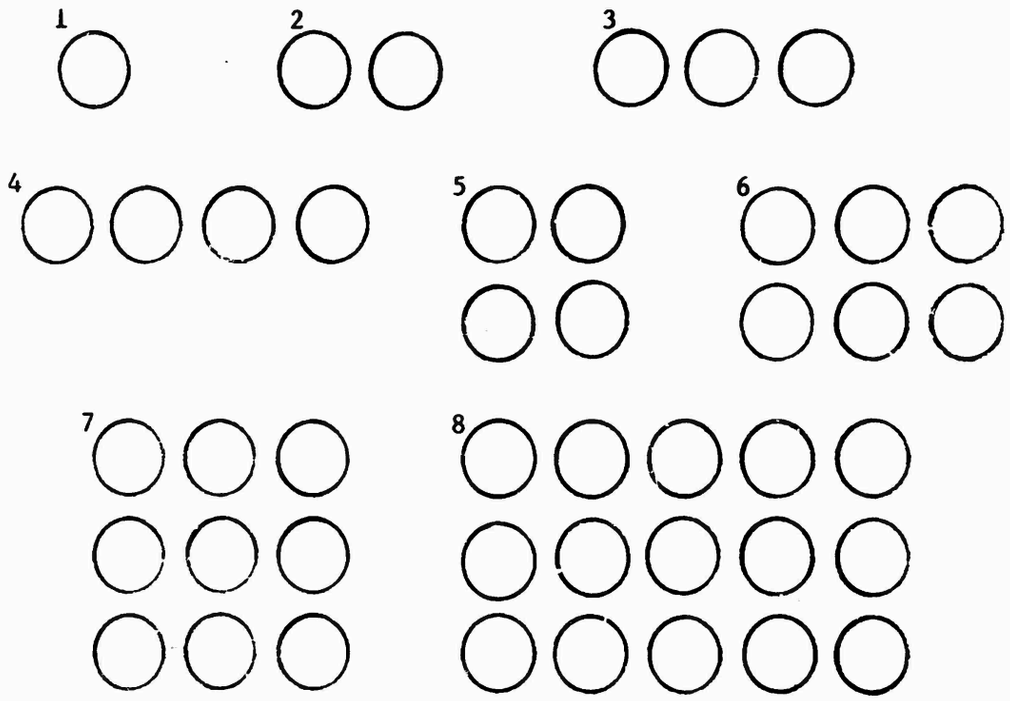

B. <u>Zero Radius Spacing</u> (r = 0)

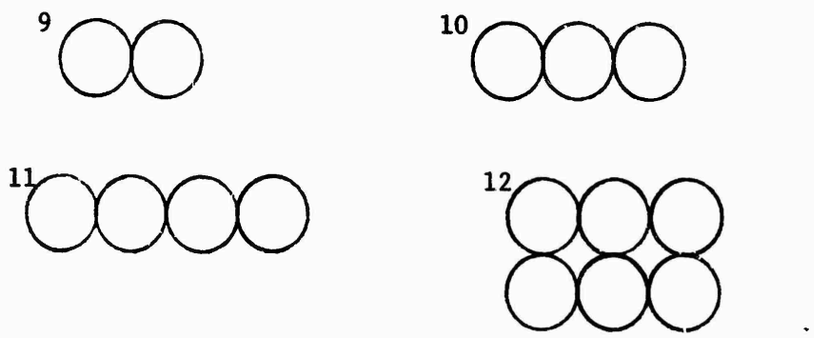

Figure 3 SMALL-SCALE MUNITION CLUSTER CONFIGURATIONS

TABLE 1

SUMMARY OF SMALL-SCALE MUNITION EXPERIMENTS

Expt. No.	Config. No.	No. of Munitions	Cluster Spacing	No. of Celotex Boxes	Arena Size (deg)	Remarks
1	1	1	-	0	90	50 gr primacord failed to initiate munition
2	1	1	-	0	90	175 gr primacord yielded proper munition initiation
3	1	1	-	0	90	Munition with 1/4 in. diam balls
4	5	2x2	1/2r	0	360	
5	6	2x3	1/2r	1	360	
6	1	1	1/2r	2	-	Celotex recovery boxes only
7	5	2x2	1/2r	3	-	Celotex recovery boxes only
8	6	2x3	1/2r	3	360	
9	2	2	1/2r	3	360	
10	3	3	1/2r	3	360	
11	9	2	0	3	360	
12	10	3	0	3	360	
13	4	4	1/2r	3	360	
14	12	2x3	0	3	360	
15	7	3x3	1/2r	3	360	
16	8	3x5	1/2r	3	360	
17	11	4	0	3	-	Celotex recovery boxes only
18	1	1	1/2r	3	90	Natural fragment cylinders
19	3	3	1/2r	3	360	Natural fragment cylinders
20	10	3	0	3	360	Natural fragment cylinders

hypothesized that the number of ball-fragment impacts on the witness sheets should be proportional to the number of models facing a defined sector of the arena. Thus, the arena sectors facing the vertical edges of the munition array were found to yield fragment counts nearly equivalent to that expected from a single munition.

The use of the Celotex fragment recovery box was initiated during Experiment 5 consisting of a 2 by 3 munition cluster. The Celotex box provided excellent data correlation with the intact fragment count obtained from the corresponding arena witness sheets. Based upon these data, all subsequent experiments incorporated three Celotex recovery boxes located 45 degrees apart to obtain fragment penetration data at the locations shown on Figure 2.

3.3.2 Data Reduction

The data obtained from the small-scale munition experiments were processed in three categories:

- Qualitative fragment interaction data were made available from photographs of the impacted witness paper.
- The high energy fragment impacts were counted on the impacted witness paper.
- The number of fragment perforations were counted on the witness paper located between each inch of Celotex in the fragment recovery boxes.

Excellent correlation was obtained from among all three data sources concerning the mechanism of fragment interaction for clustered munition models.

The photographic data from the impacted witness paper were used to reconstruct the explosive arena. To obtain these data, a 4 by 4 ft light stand was constructed with fluorescent illumination sources. The witness paper was back-lighted and photographed with the camera adjusted to expose the fragment impact perforations. The composite witness paper photographs provided qualitative evidence that simultaneous detonation of the munition cluster was achieved as indicated by the regular cyclic patterns among the shattered and intact fragment impact zones of the arena.

Quantitative fragment interaction data were obtained from the high-energy fragment impact counts for each 11.25 degree sector of the arena. The high energy fragment was arbitrarily defined as any ball-fragment perforation which projected an area greater than one-half that of a 3/16 in. diameter sphere. To obtain these data, the arena witness sheets were selected in random order and placed on the fluorescent light stand equipped with grids to facilitate the fragment count process. The counts obtained were coded and deciphered as a separate operation to assure unbiased numerical values.

The three Celotex collection boxes located 45 degrees apart behind the plywood witness sheets provided useful information concerning fragment impact density and penetration energy for each munition cluster considered. For each collection box, the number of fragment perforations were counted for each inch of Celotex thickness. From these data, the number of fragments penetrating 5 inches of Celotex was compared with the corresponding witness paper count on an equivalent area basis. The count of these fragment perforations showed good correlation with data obtained from high-energy fragment counts obtained from the corresponding arena sector. The Celotex collection boxes also provided conclusive evidence that the fragment velocity is increased by some factor proportional to the number of munitions considered in the cluster.

Three experiments were conducted using naturally fragmenting cylinders. The steel cylinders were designed to simulate the performance characteristics of the ball-type, preformed-fragment explosive models. A comparative examination of the experimental results from the two munition designs with similar cluster configurations verified that the mechanism of fragment interaction and distribution is similar in behavior. The recovered fragment samples from the natural cylinder indicated that the average fragment weight was about 12 grains, while the reference 3/16 in. diameter steel ball weighed about 7 grains. It was inferred from these data that the fragment interaction phenomena associated with the current ball-type munition model, correlates with configurations found in conventional ordnance items. It should be emphasized that these relationships are valid only if the comparative munitions have similar distributions of explosive charge and metal.

3.3.3 Analysis of Small-Scale Experiments

Fragment impact data obtained from the arena witness paper, were utilized to obtain a quantitative measure of the distribution of fragments around the arena. Figures 4 through 6 present the number of fragments collected at each of the 32 intervals of 11.25 degrees around the arena. It is readily apparent that in zones where interaction of fragments takes place that a concentration or enhancement effect takes place. In the zones where the ball bearings do not interact in flight, their behavior is similar to that expected from a single munition. It can also be observed from the figures that enhancement is concentrated over discrete ranges of sector angle. Both the magnitude of enhancement and the degree of sector angle concentration is seen to be dependent on the spacing of the munitions. The enhancement or amplification of the number of fragments were found principally in a narrow band of $\pm$ 11-1/4 degrees about the normal to the stack. This increase in number dropped off to about one-fourth the difference between the maximum amplification factor and the fragment count from a single munition in a zone of 11-1/4 to 22-1/2 degrees from the normal to the stack. In the next zone from 22-1/2 to 45 degrees, the fragment count was due only to a single munition. The enhancement zone for zero spacing is much narrower and only shows an amplification factor at $\pm$ 11-1/4 degrees; dropping off to unity at all other zones. The maximum amplification factors in the region $\pm$ 11-1/4 degrees about the normal to the stack is shown in Figure 7 in terms of the dimensions of the stack (i.e., number of units in a row (N) and the height of the stack (M)). The munition spacing factor r is expressed in number of radius.

In the small-scale experiments, on which the amplification factors are based, the fragment count was determined by counting the number of holes that were produced by fragments that were greater than one-half of their original size. This criterion was used because collisions between fragments resulted in breakup of fragments. In Figure 7, the curve for r = 0 shows higher amplification factors than for the r = 1/2 spacing between munitions. This was due to the fact that there are more fragment interactions in the closer spaced munitions and hence more broken fragments, resulting in a larger count. A general formula for amplification factors (AF) was derived for a stack greater than 2 x 2 and is presented as:

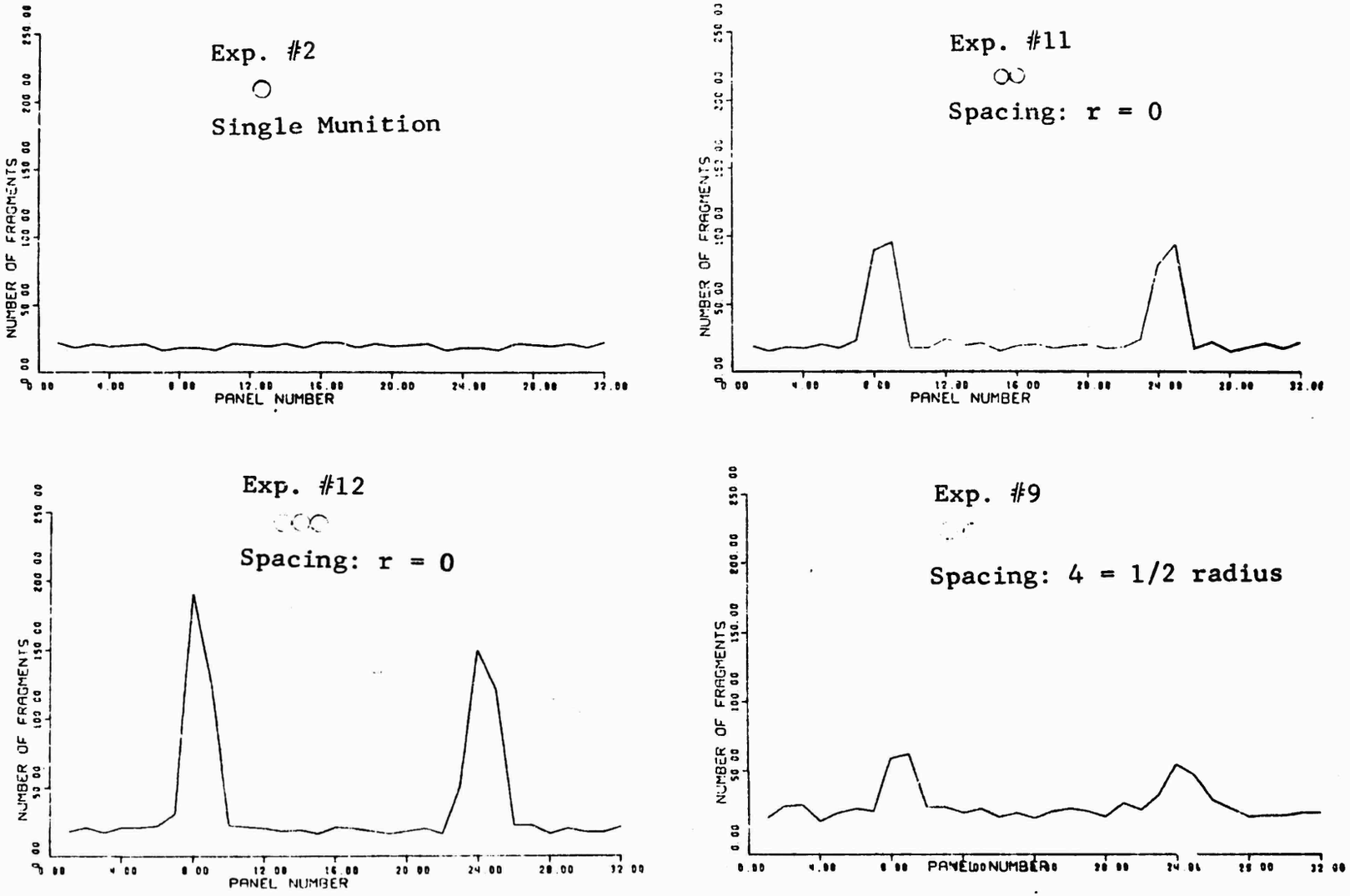

Figure 4 FRAGMENT COUNT AT PANELS (11.25 deg Intervals)

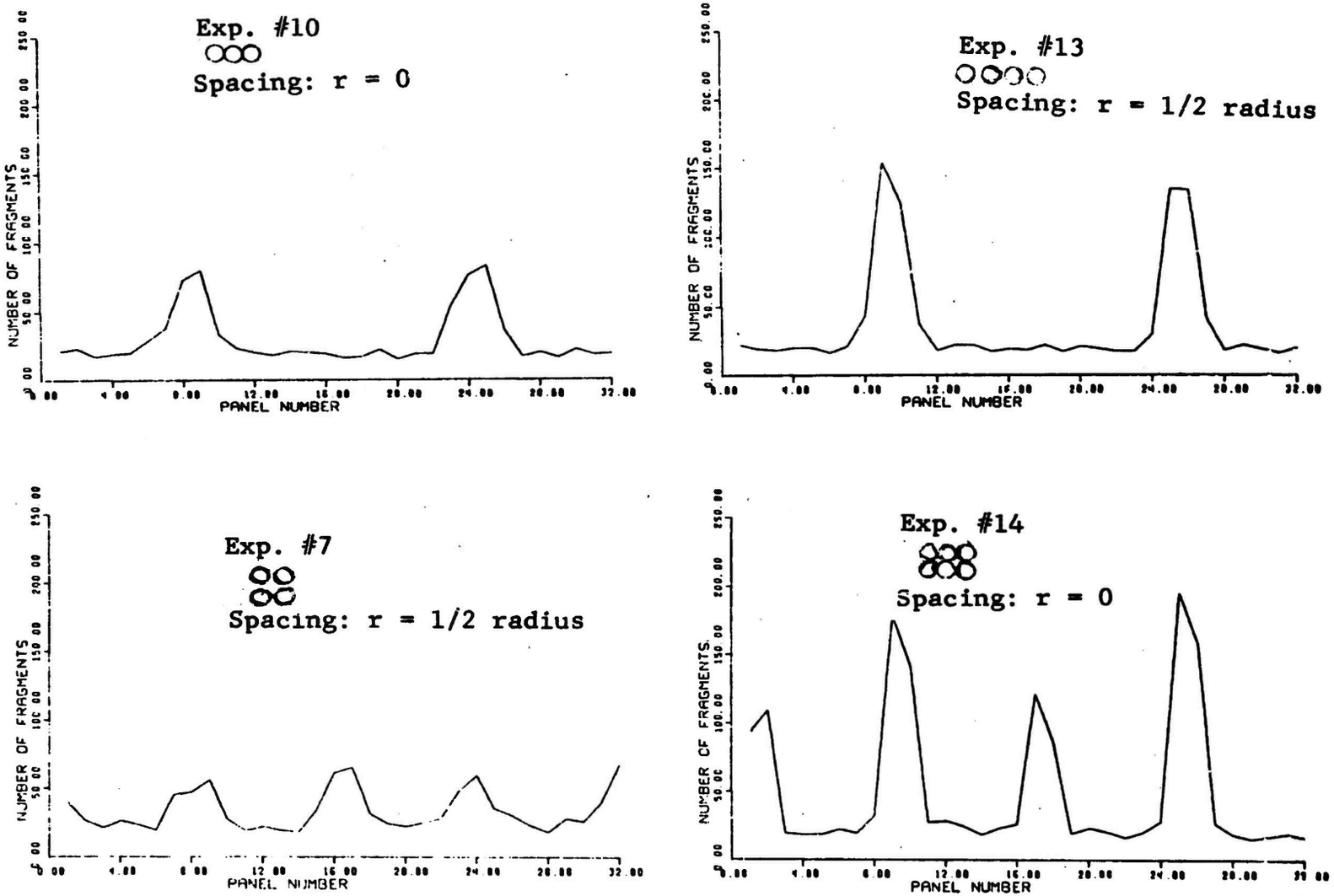

Figure 5 FRAGMENT COUNT AT PANELS (11.25 deg Intervals)

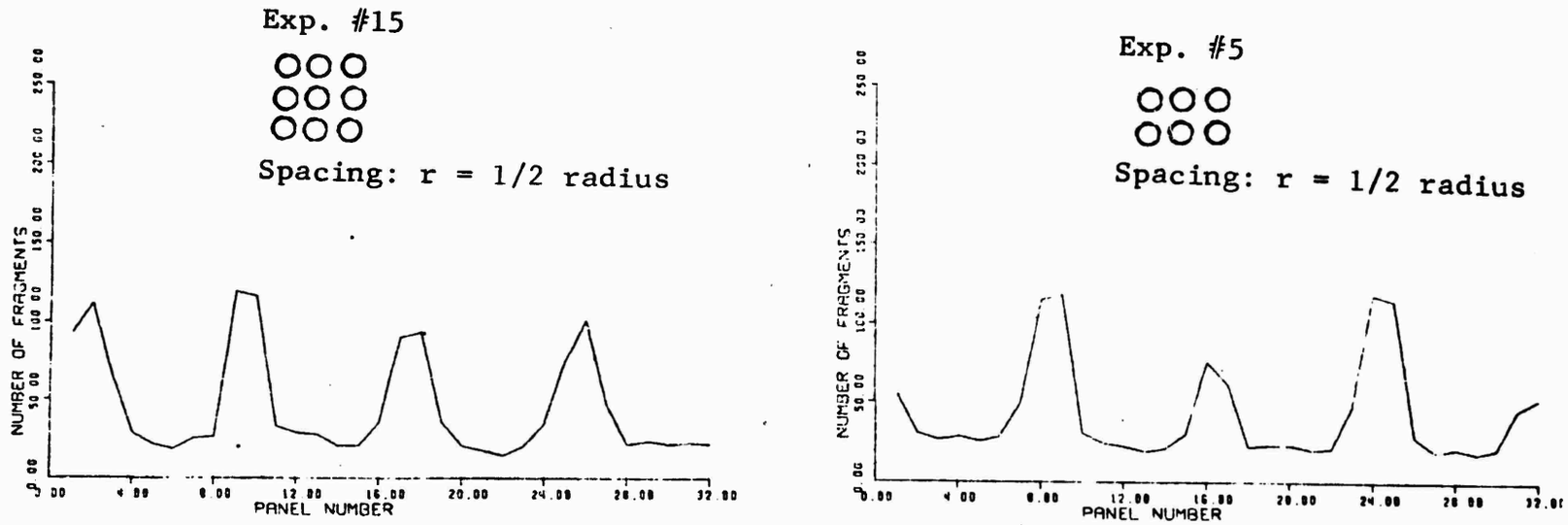

Figure 6 FRAGMENT COUNT AT PANELS (11.25 deg Intervals)

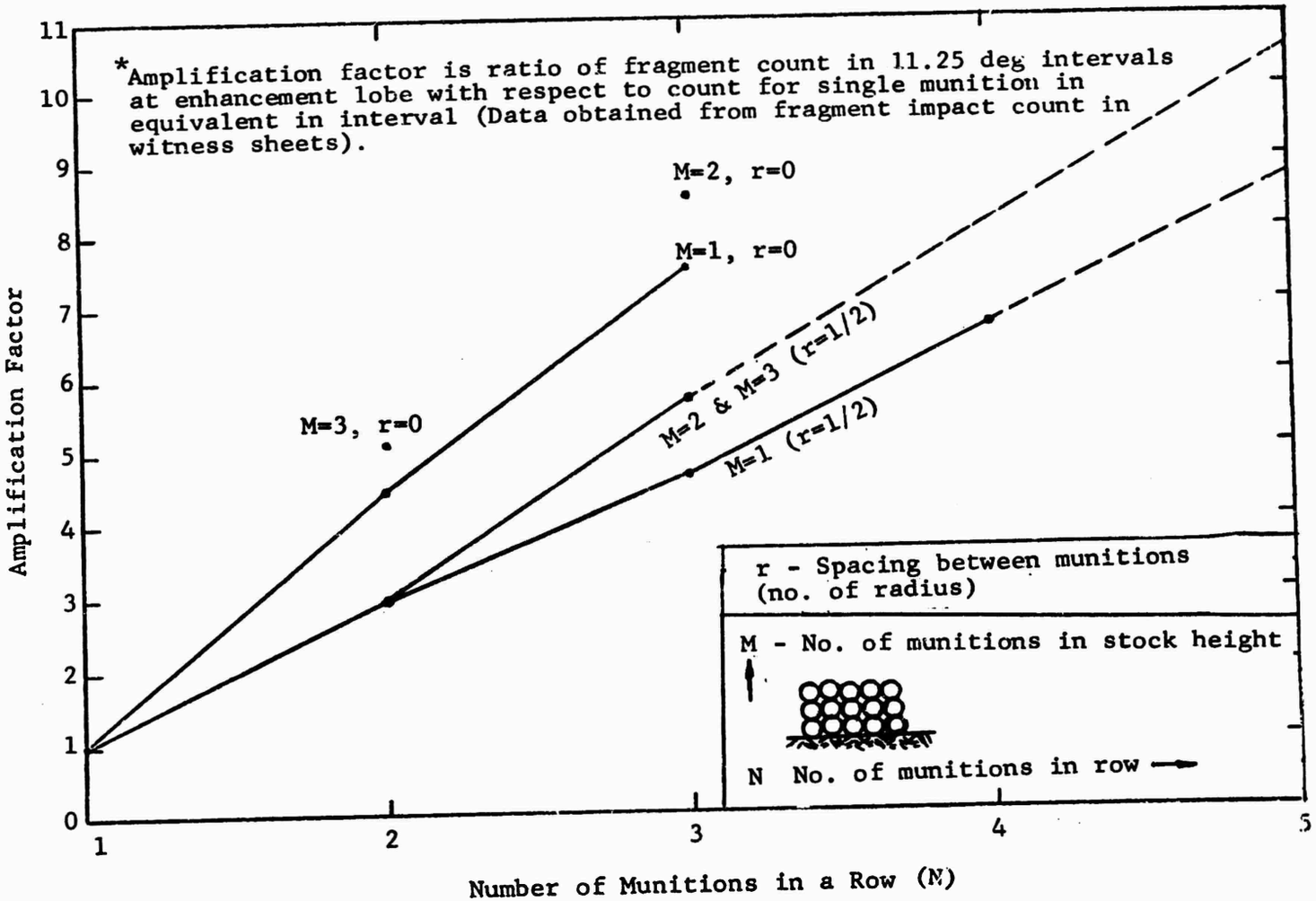

Figure 7 AMPLIFICATION FACTORS FOR VARIOUS MUNITION CONFIGURATIONS

$$AF_{r=1/2} = 5.8 + 2.4\ (N-3) \text{ for } N \geq 3$$

$$AF_{r=0} = 8.5 + 3.7\ (N-3)$$

These equations are for a region of $\pm$ 11-1/4 degrees. From 11-1/4 to 22 degrees:

$$\overline{AF} = \frac{AF - 1}{4} + 1$$

Although a 3 x 5 munition cluster is included in the small-scale test series, it resulted in sufficient blast pressures to obscure the witness paper and thus enhancement rules were not directly available for this munition cluster. The relationship defined in Figure 7, however, was utilized to obtain an estimate of the enhancement and this estimate was used in the analytic model to obtain comparisons with the corresponding full-size test at NWC. Judging from the results of this comparison, material enhancement and munition cluster configuration are directly related.

Table 2 summarizes the recovery data for different cluster configurations. It is apparent that the percent of balls recovered is related to the amount of shading taking place between munitions in the cluster. A simple geometric model of shading, which allows for enhancement effects to take place, is shown in Figure 8. Here, the measure of fragment performance was exposed circumference. The exposed circumference was defined by drawing tangent lines from the center of each munition to the top and bottom of each adjacent munition. When radii are extended to intersect these tangent lines and two chords are extended between the four intersection points a hexagon is defined. This hexagon defines an area where total shading takes place. That portion of the munition cross-sectional circumference outside the shaded region is defined as the exposed circumference. Figure 9 shows the relationship between the exposed circumference and the number of balls recovered for 10 different munition configurations. The relationship is suprisingly regular and tends to confirm the regularity which was found to exist in Figure 7.

TABLE 2

SUMMARY OF SMALL-SCALE TEST RESULTS FOR DIFFERENT CLUSTER CONFIGURATIONS

CONFIGURATIONS	o	oo	o o	ooo	o o o o	o o o o	888	o o o o o o	o o o o o o o o o
BALLS FOUND	620	884	791	1168	934	1065	1591	1347	1433
BALLS AVAILABLE	675	1350	1350	2025	2025	2700	4050	4050	6075
PERCENT RECOVERY	91.8	65.5	58.6	57.7	46.1	42.9	39.3	33.3	23.6

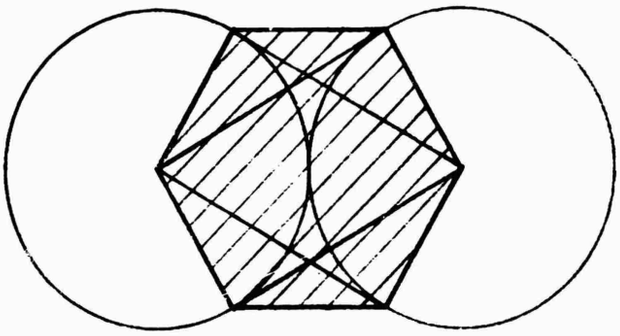

A. Zero Spacing between Munitions (r=0)

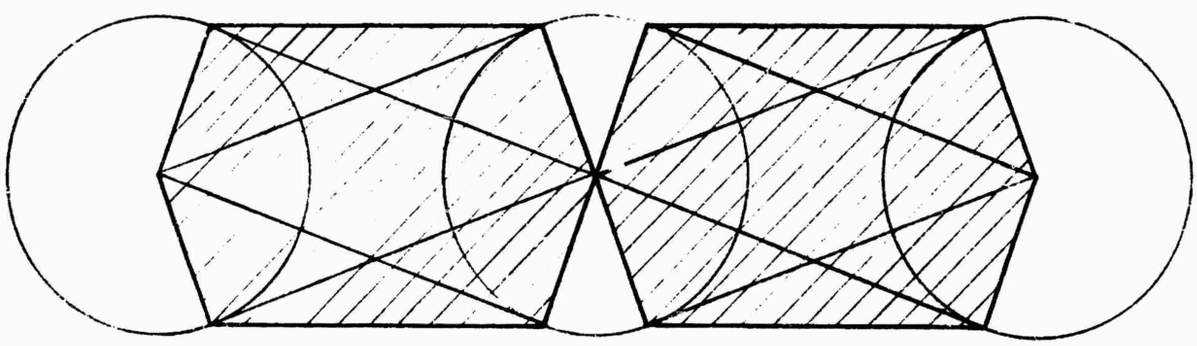

B. One-half Radius Spacing between Munitions (r = 1/2)

Figure 8 SIMPLE GEOMETRIC SHADING MODEL

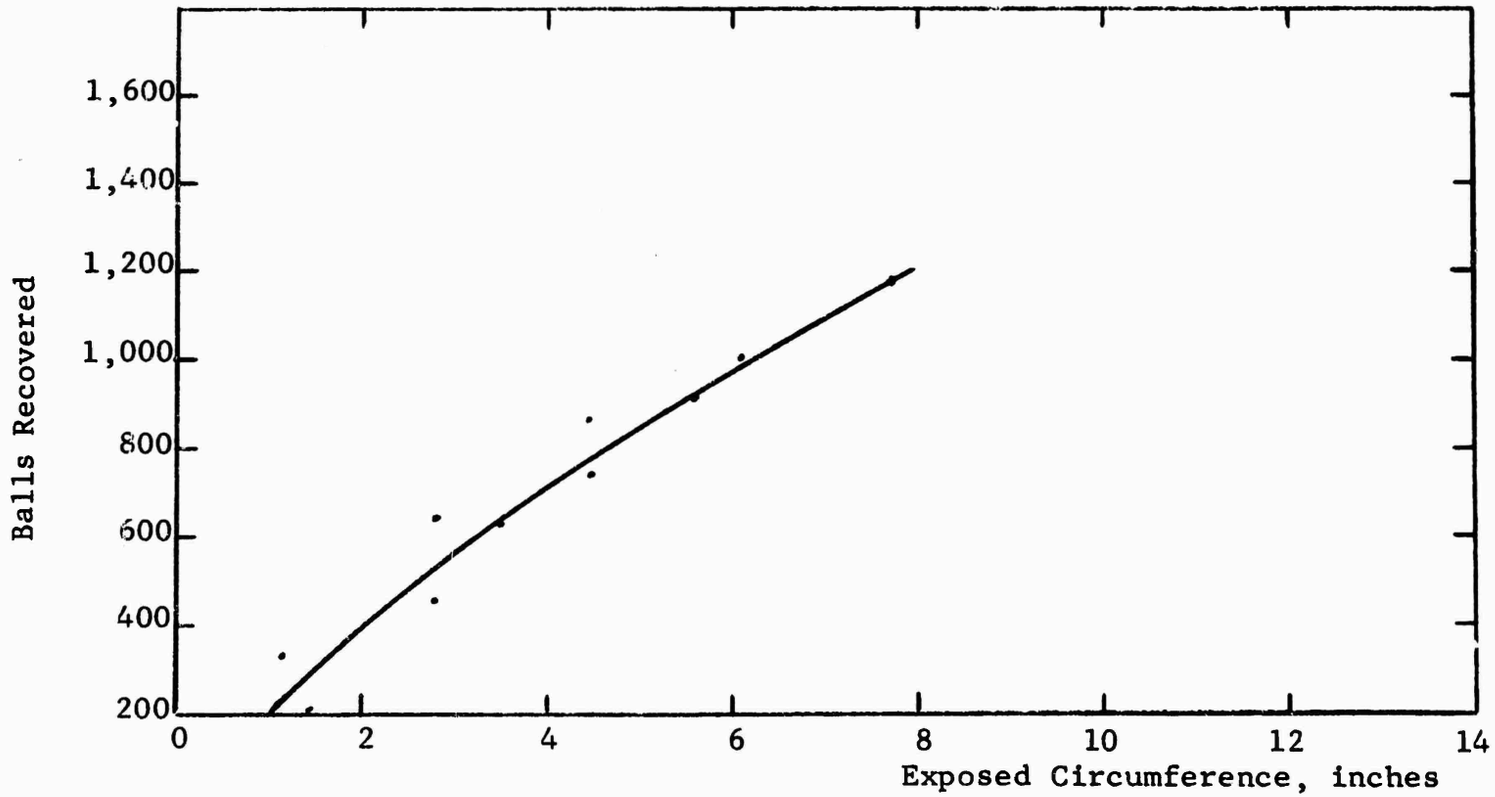

Figure 9 NUMBER OF BALLS RECOVERED AS A FUNCTION OF EXPOSED CIRCUMFERENCE

Although attempts have been made, no fundamental understanding of the enhancement effect has been achieved. The above geometric model allows for interaction of fragments, and hence enhancement, to take place in zones where this effect has been observed experimentally. This interaction occurs somewhat down range of the stack position and is a random phenomenon. This has been confirmed by examining recovered material in the recovery boxes. The balls from a single munition do not interact and were observed to be generally intact whereas many of the balls from clusters of munitions, in the zones of enhancement, were observed not to remain intact. Enhancement rules which are currently being used, therefore, are empirical rather than theoretically deduced interaction rules and are summarized in Figure 7.

Table 3 summarizes the small-scale Celotex recovery box data. This table gives the number of balls penetrating each of up to 10 1-in. layers of Celotex. Boxes were stationed at 0, 45, and 90 degrees with respect to munition stack configurations, (see arena schematic on Figure 2).

The maximum amplification factors for fragments greater than one-half their original size can be compared with the Celotex recovery box data. These data, coupled with visual observations, show that the decrease in numbers of fragments penetrating the successive layers of Celotex is due to the fact that there are a large number of small fragments that are caught in the first four or five layers. Only the largest fragments (i.e., those not encountering collisions) are fast enough to penetrate layer 5. In the case of a single munition, where all the fragments remain intact, an average of 11 fragments penetrate layer 5. In the case of r = 1/2 spacing between munitions, a row of two munitions, in any stack configuration, results in an average of 22 fragments penetrating layer 5. Similarly, stacks of three and four munitions result in an average of 34 and 51 fragments, respectively, collected in the direction normal to the stack row. Thus, amplification factors for intact (i.e., fast) fragments, in the direction of maximum concentration, are a multiple of the numbers of munitions in a row, up to four in a row.

There is a decrease in the large size fragments passing through layer 5 for the case of five munitions in a row. In this case 31 fragments pass through layer 5. This is probably due to a greater collision probability associated with a larger number of munitions. Thus, the amplification factor for large intact fast fragments seems to level off at about a value of AF = 3.

For the case of zero spacing between munitions the amplification factor, for large fragments, appears to be insensitive to the number of munitions in a row. For two and three units in a row, the amplification factor in the direction of maximum concentration is 2. For four units in a row the amplification factor is 2.5. Thus the zero spacing shows saturation at a smaller stack size and has a lower amplification factor.

The small-scale Celotex recovery box data, Table 3, shows some additional penetration of Celotex by fragments originating in the larger stacks. This implies that there is an increase in initial velocity when there is more than a single munition. For a single munition about 25 percent of the fragments penetrating layer 5 have sufficiently high residual velocity to penetrate layer 6. For any stack, however, with two or more munitions, an average of 75 percent of the fragments which penetrate layer 5 have sufficiently high residual velocities to penetrate layer 6. Similarly, for a single munition no fragments pass through layer 7; however, for three or more munitions, an average of 30 percent of the fragments that penetrate layer 5 also penetrate layer 7. These additional two layers of Celotex represent a 20 percent increase of penetration for 30 percent of the intact fragments originating in stacks of three or more munitions. This increase in penetration is due to an increase in initial velocity of the order of 10 percent.

TABLE 3

SMALL-SCALE CELOTEX RECOVERY BOX DATA

Config.	Angle	Number of balls through sheets (in.) 1	2	3	4	5	6	7	8
	90°	12	12	12	12	12	4		
o	45°	12	12	12	12	12			
	0°	9	9	9	9	9	2		
90° ↑ 45°	90°	48	31	27	25	24	18	2	
o o→ 0°	45°	16	16	15	14	12	9		
Orientation	0°	15	15	15	15	10	6	1	
	90°	28	26	23	23	23	20	2	
oo	45°	12	12	12	11	10	6		
	0°	11	11	11	11	11	6		
	90°	54	42	34	28	22	15		
ooo	45°	13	13	11	11	11	6		
	0°	17	15	14	13	11	4		
	90°	77	52	40	36	31	25	6	
o o o	45°	23	20	18	12	12	10	1	
	0°	12	12	12	10	8	3		
	90°	61	38	33	26	26	14		
o o	45°	15	15	15	15	14	10		
o o	0°	44	28	27	23	20	11		
	90°	83	53	46	35	34	25	2	
o o o	45°	12	12	12	12	12	7	0	
o o o	0°	33	25	22	18	17	11	0	
	90°	145	81	41	31	26	22	12	
888	45°	13	13	12	12	12	12	0	
	0°	111	58	35	30	24	17	4	
	90°	117	69	46	39	35	28	9	
o o o	45°	15	13	12	12	12	7	1	
o o o	0°	157	88	58	53	45	35	15	1
o o o									
	90°	155	97	71	59	51	35	5	
o o o o	45°	14	14	14	14	14	11		
	0°	13	13	13	13	13	5		
o o o o o	90°	110	67	47	39	31	25	13	1
o o o o o	45°	17	15	11	11	10	9	1	
o o o o o	0°	46	33	31	26	25	17	6	
	90°	131	79	53	38	30	21	10	
oooo	45°	15	15	14	14	13	12	4	
	0°	16	16	16	16	16	15	9	

4. M117 BOMB STACK EXPERIMENTS

As part of a coordinated effort to investigate the hazards associated with fragments from stacked munitions in open store, an experimental program was designed to obtain farfield fragment data from stacked M117 bombs. Previously, small-scale munition experiments were conducted to generate fundamental information concerning the initial fragment field, utilizing parameters associated with the planned M117 bomb stack experiments. These data served as the frame of reference for assessing the results of the full-scale experiments. The Naval Weapons Center (NWC) at China Lake, California was selected as the test site because of its suitable terrain and the availability of ancillary equipment to conduct controlled munition experiments and to recover bomb fragments from relatively large collection areas.

4.1 M117 A1E1 Bomb Stack Configurations

The two configurations used in the M117 bomb stack experiments are illustrated on Figures 10 and 11. The first test consisted of six bombs stacked three high and two wide, while the second test consisted of 15 bombs stacked three high and five wide. The bombs were stacked on 4 by 4 in. timbers between each layer, and chocked with 2 by 4 in. lumber to maintain the 4 in. spacing between the rows of bombs. The specification above corresponds to the one-half radius munition spacing which was a key parameter in the small-scale experiments. The munition specifications are:

Type: 750 lb general purpose bomb
Model: M117 A1E1
Lot Number: 1325-143-6981-F116
Manufacturing Date: June 1969

These bombs were provided without fuzing or tail fin assembly. Approximately 50 percent of the total bomb weight is tritonal explosive charge.

An important consideration regarding the M117 bomb stack experiments is the rationale supporting the two configuration test series. The first test configuration of six bombs stacked three high and two wide has all bombs yielding some measure of unobstructed side-spray fragments. The second configuration of 15

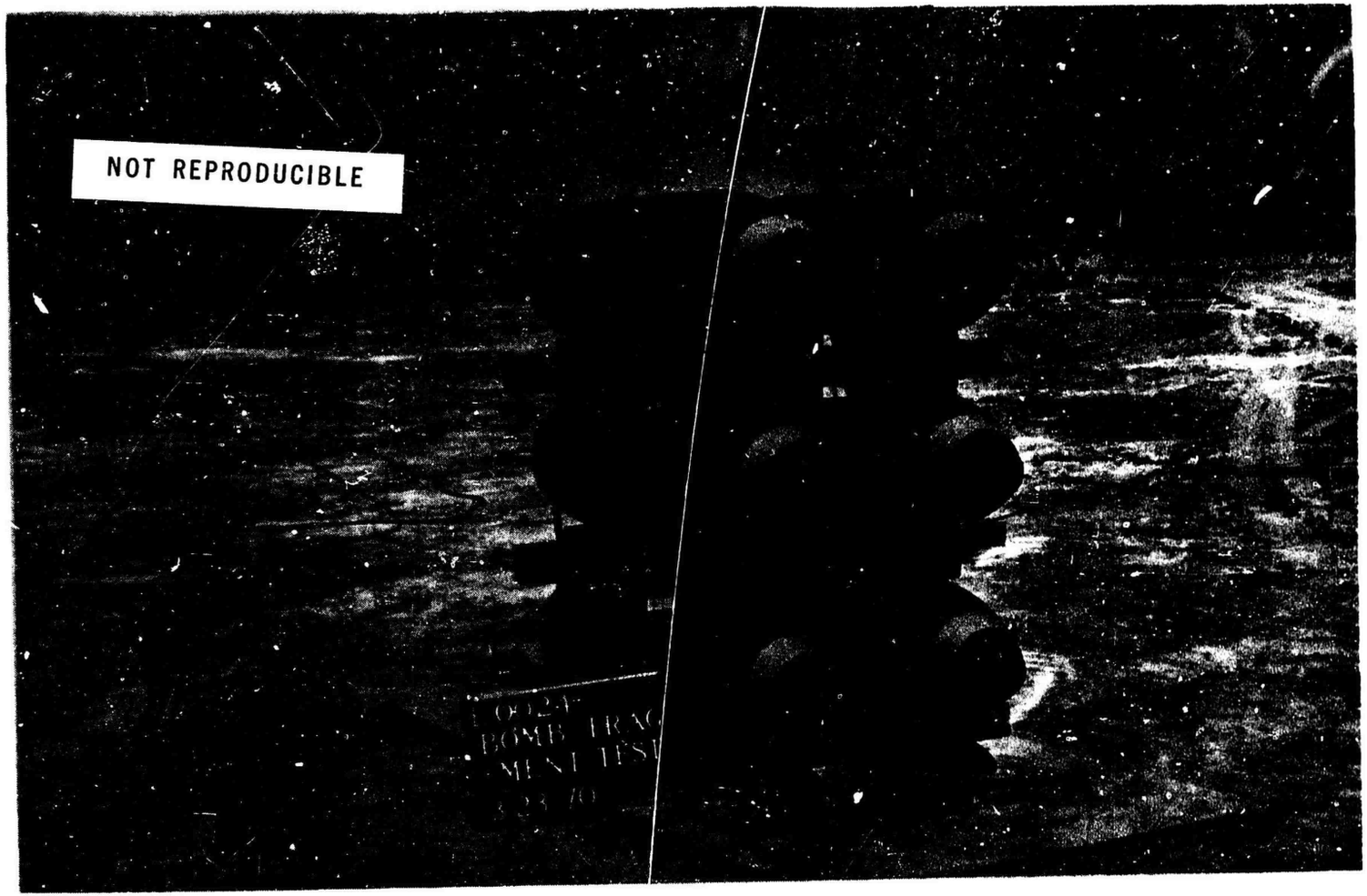

Figure 10 SIX-BOMB STACK CONFIGURATION (3x2) AT NWC-CHINA LAKE

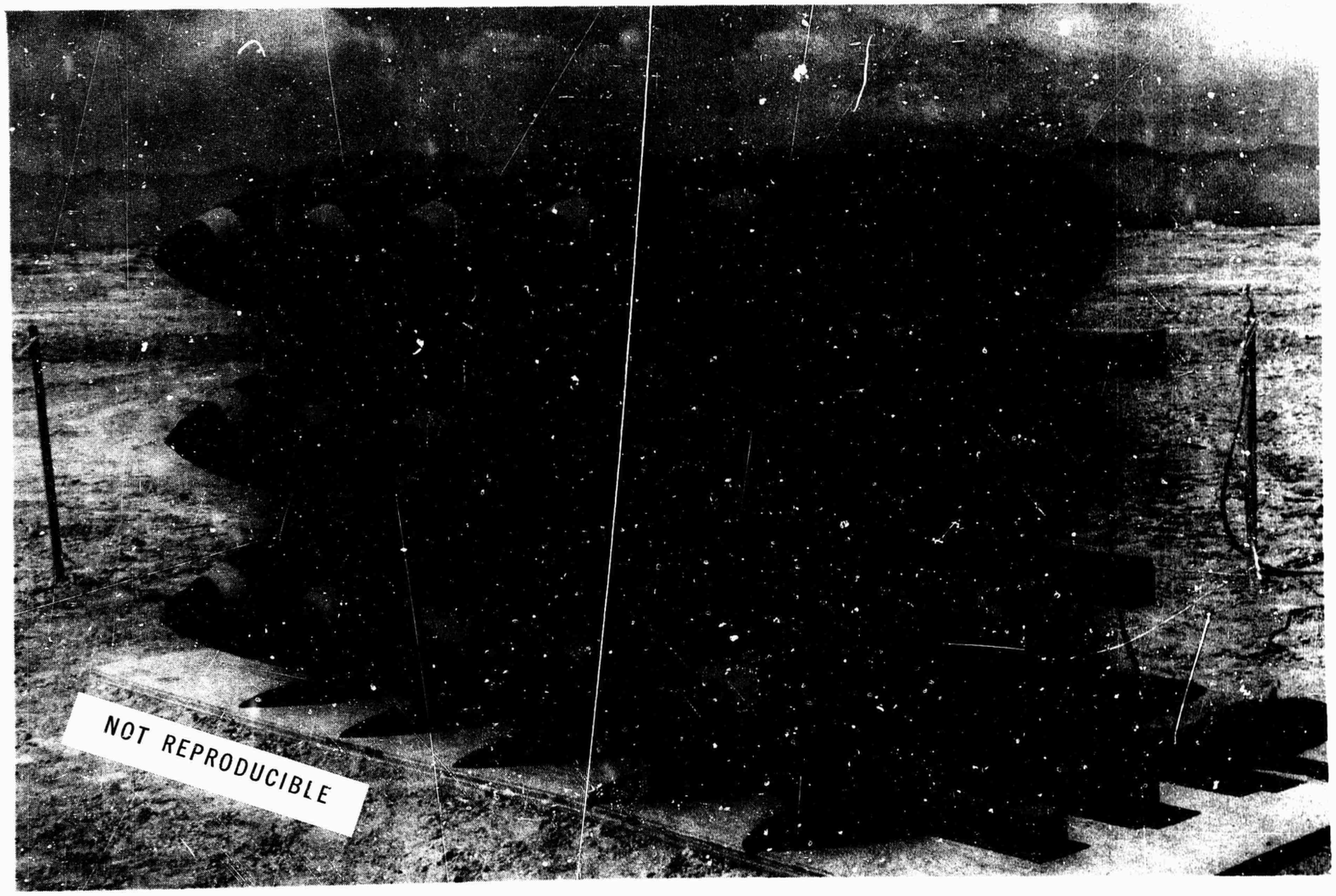

Figure 11 FIFTEEN-BOMB STACK CONFIGURATION (3x5) AT NWC-CHINA LAKE

bombs stacked three high and five wide has six bombs completely masked by the peripheral munitions. Useful fragment interaction data was expected regarding the effect of stack length and the relative effectiveness of the fully masked bombs. The small-scale experiments have yielded data providing additional rules for clustered munitions and initial fragment interference effects. These full-scale tests were designed to provide farfield fragment distribution data which could be used to verify information generated by the small-scale experiments.

The M117 bomb stacks were detonated simultaneously to facilitate data comparison with the small-scale tests. This was accomplished by attaching equal length primacord to the base fuze well of each M117 bomb and detonating the clustered free ends of the prima cord with a single detonator supplemented with C-4 explosive charge.

4.2 Fragment Collection Technique

The basic fragment collection cell specifications were designed to complement numerical data obtained from analytical methods used to compute fragment number and mass densities for projected range of M117 bomb fragments. The fragment collection cell specifications as applied to the M117 bomb stack experiments are illustrated on Figure 12. The eight-spoke fragment collection network provides pie-shaped sectors which subtend an angle of 8 degrees 36 min spaced 45 degrees apart. Each sector was divided into eight cells starting from 500 ft and extending to 2000 ft distances measured along the radial borders originating at the bomb stack. Starting at the 500 ft mark, two consecutive cells with the following radial sides are listed in order: 100, 150, 200 and 300 ft. The line drawn across the 500 ft points of the sector radial border is 75 ft, while the line across the 2000 ft points are 300 ft. This network provides a total of 64 distinct collection cells for each experiment.

The fragment collection cells as specified in Figure 12, were surveyed and staked with flags to facilitate identification by the fragment collection vehicle. The collection sectors were leveled and cleared of all scrub vegetation and fragment debris prior to the experiment. The bomb stack site was also surveyed to assure proper alignment between the bomb stack and the fragment collection network.

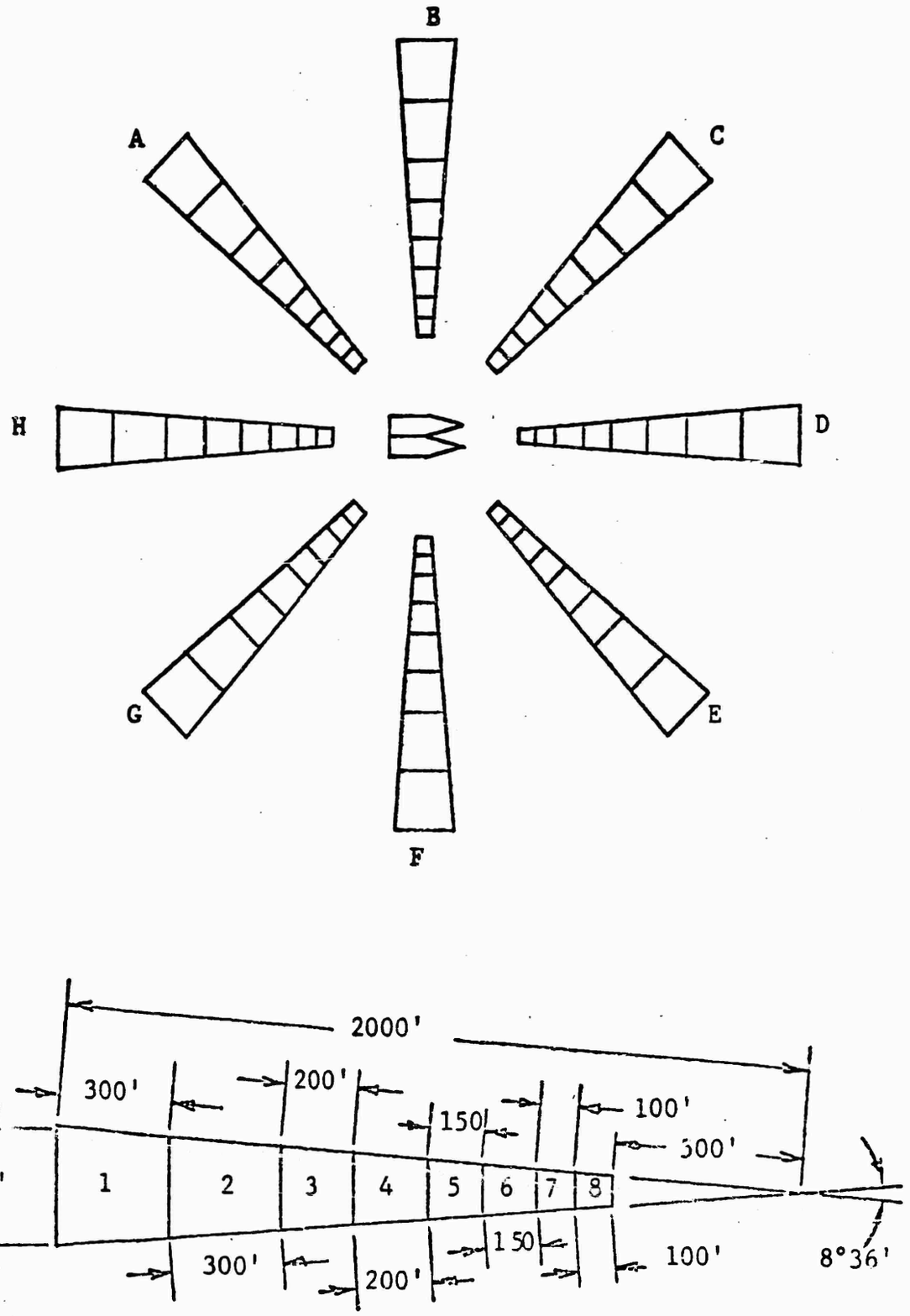

Figure 12 NWC FRAGMENT COLLECTION CELL SPECIFICATION

After each of the two bomb stacks were detonated, a truck-mounted electromagnet shown on Figure 13, was used to collect the bomb fragments in each of the 64 collection cells in a manner analogous to plowing a field. At suitable intervals, the underslung vehicle magnet was parked over a canvas cloth to deposit fragments as shown on Figure 14. The cloth full of fragments was then pulled from under the vehicle, which permitted the fragment collection process to resume with a minimum of delay. The fragments were then transferred to a plastic sandbag and tagged with the appropriate cell identification number. Visual inspection of the cleared fragment cells indicated that the magnet did a thorough job of picking up the significant fragments providing that the vehicle speed was kept below 2 miles per hour. The fragments collected from the two experiments were shipped to IITRI for data processing and analyses.

4.3 Supplementary Data

To complement the two M117 bomb stack experiments, meteorological data was recorded during each test to document surface weather conditions and the weather aloft up to 5,000 ft altitude in 200 ft increments. These data indicated that the wind velocity did not exceed 12.2 knots. It may be concluded that the meteorological conditions had an insignificant effect on the ballistic trajectories of the bomb fragments.

Two Hycam 16mm cameras were used with color film to document the detonation of the stacked bombs with film speeds about 10,000 and 4,000 fps, respectively. A review of these films, as viewed from the primed base ends of the bombs, indicated that the bomb stack had detonated simultaneously as required, based upon the symmetrical shape of the initial fireball.

A 4 by 5 in. still camera and a 16mm movie camera were used to describe the overall experimental procedure and posttest results. As a special task, a qualitative sample of side-spray fragments were documented with photographs using a 35 by 35 ft cell size located adjacent to the surveyed fragment collection cells. A representative sample of these data are shown on Figures 15 through 18, as taken from the 15 bomb tests for Cell 4 (1000 to 1200 ft from ground zero). These data illustrate: (a) 14 fragments were collected

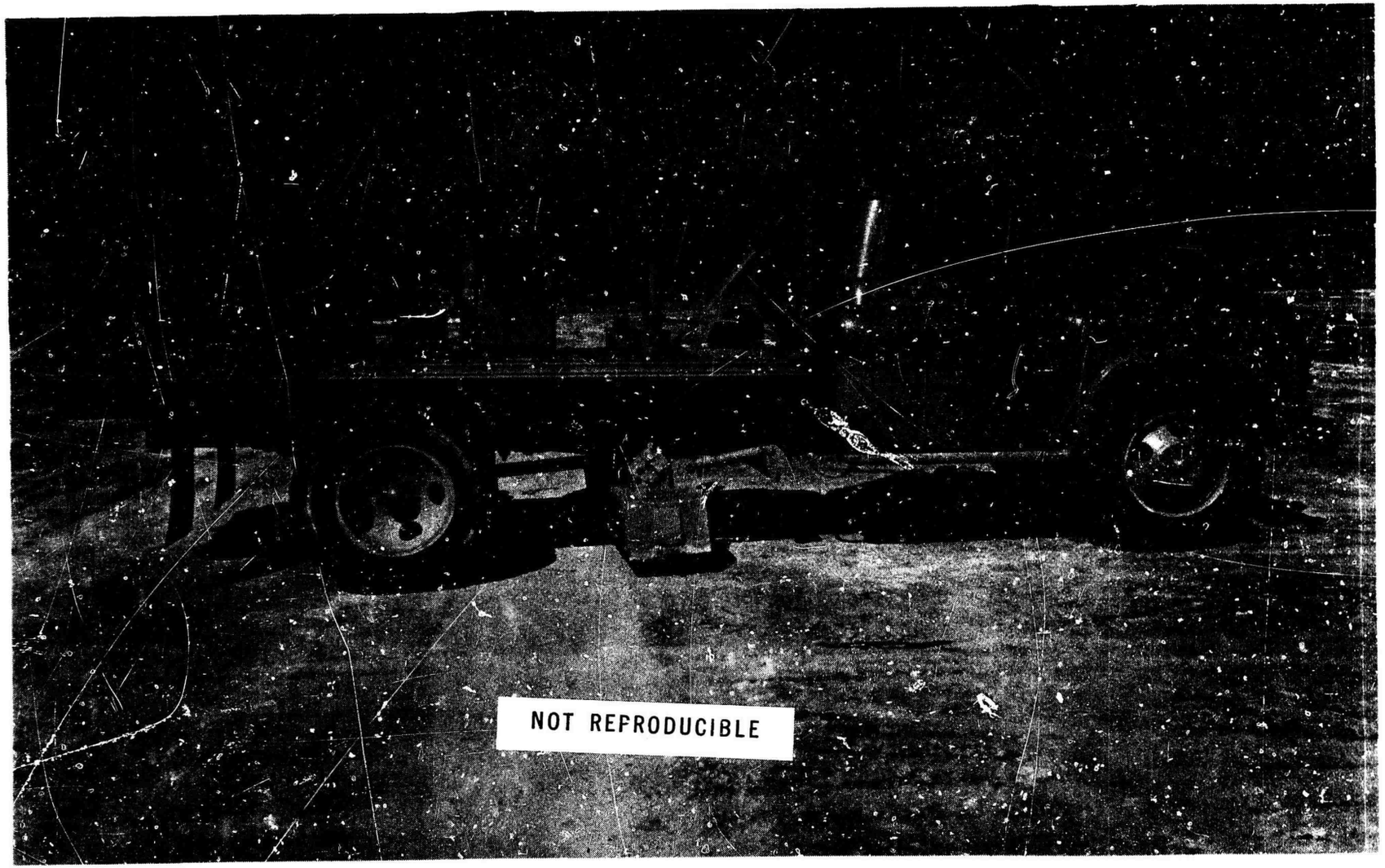

Figure 13 NWC TRUCK-MOUNTED ELECTROMAGNET USED FOR COLLECTING M117 BOMB FRAGMENTS

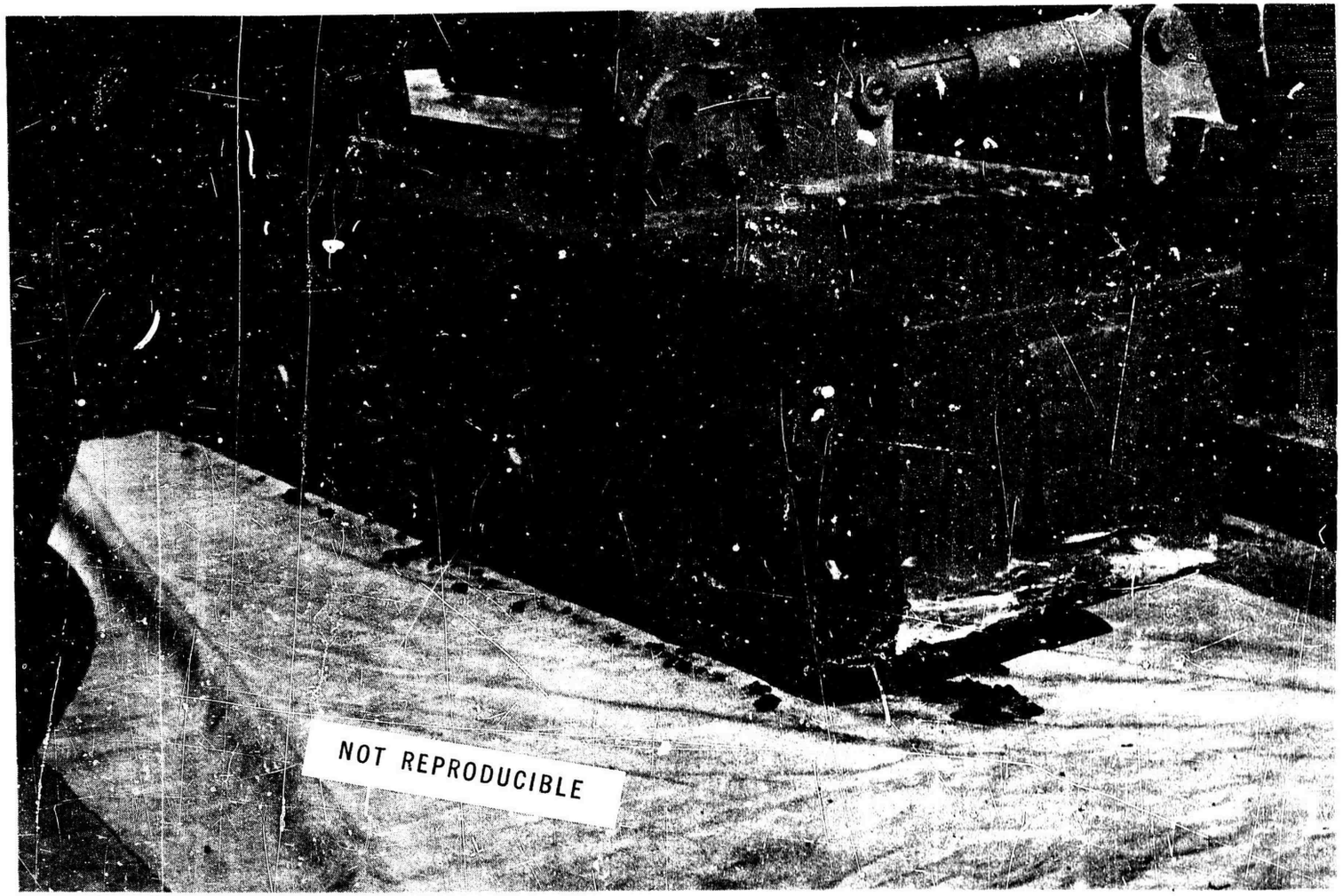

Figure 14 APPLICATION OF CANVAS CLOTH TO COLLECT FRAGMENTS FROM ELECTROMAGNET

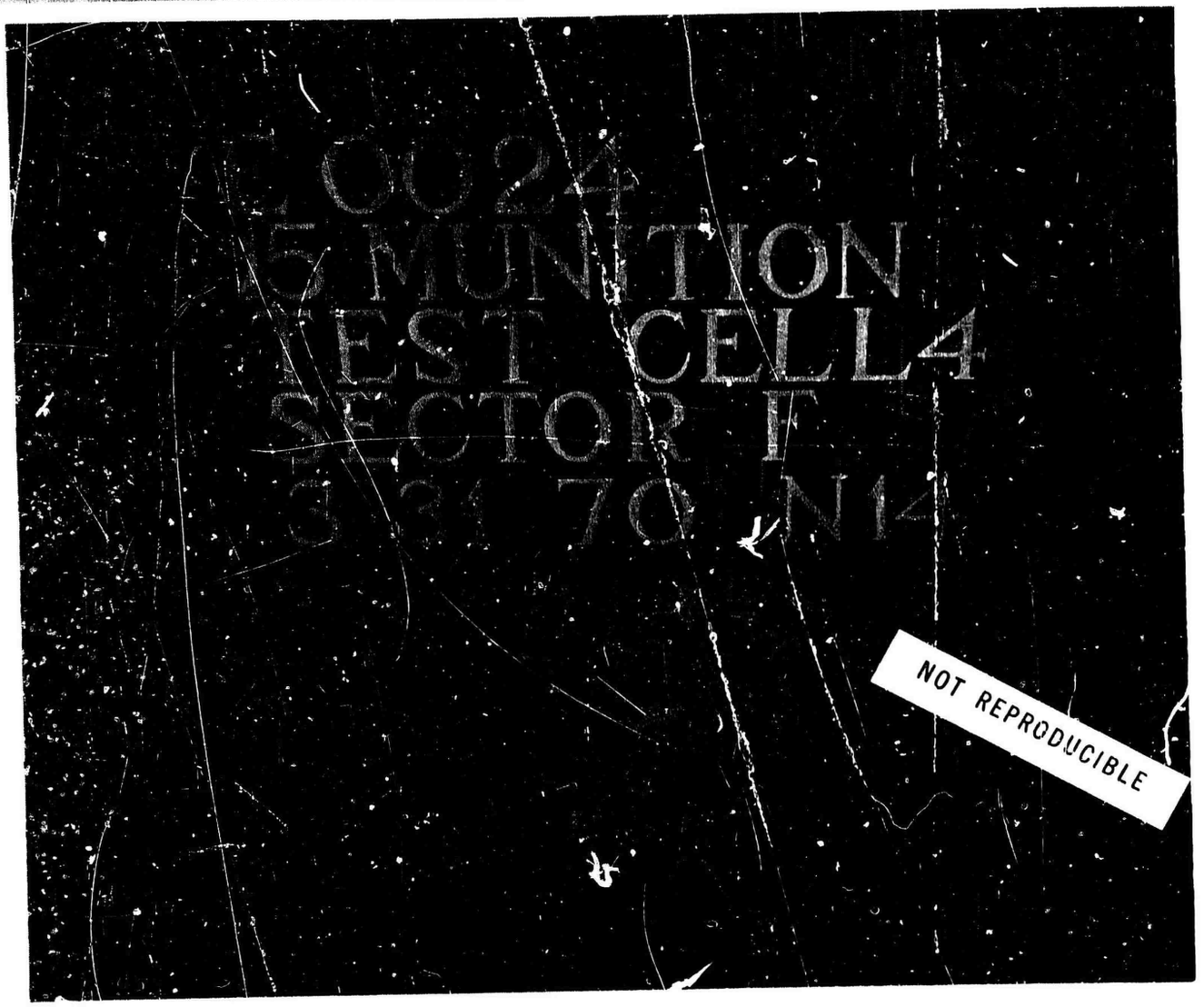

Figure 15 REPRESENTATIVE BOMB FRAGMENTS (SIDE SECTOR F, CELL 4) FROM 15 BOMB STACK

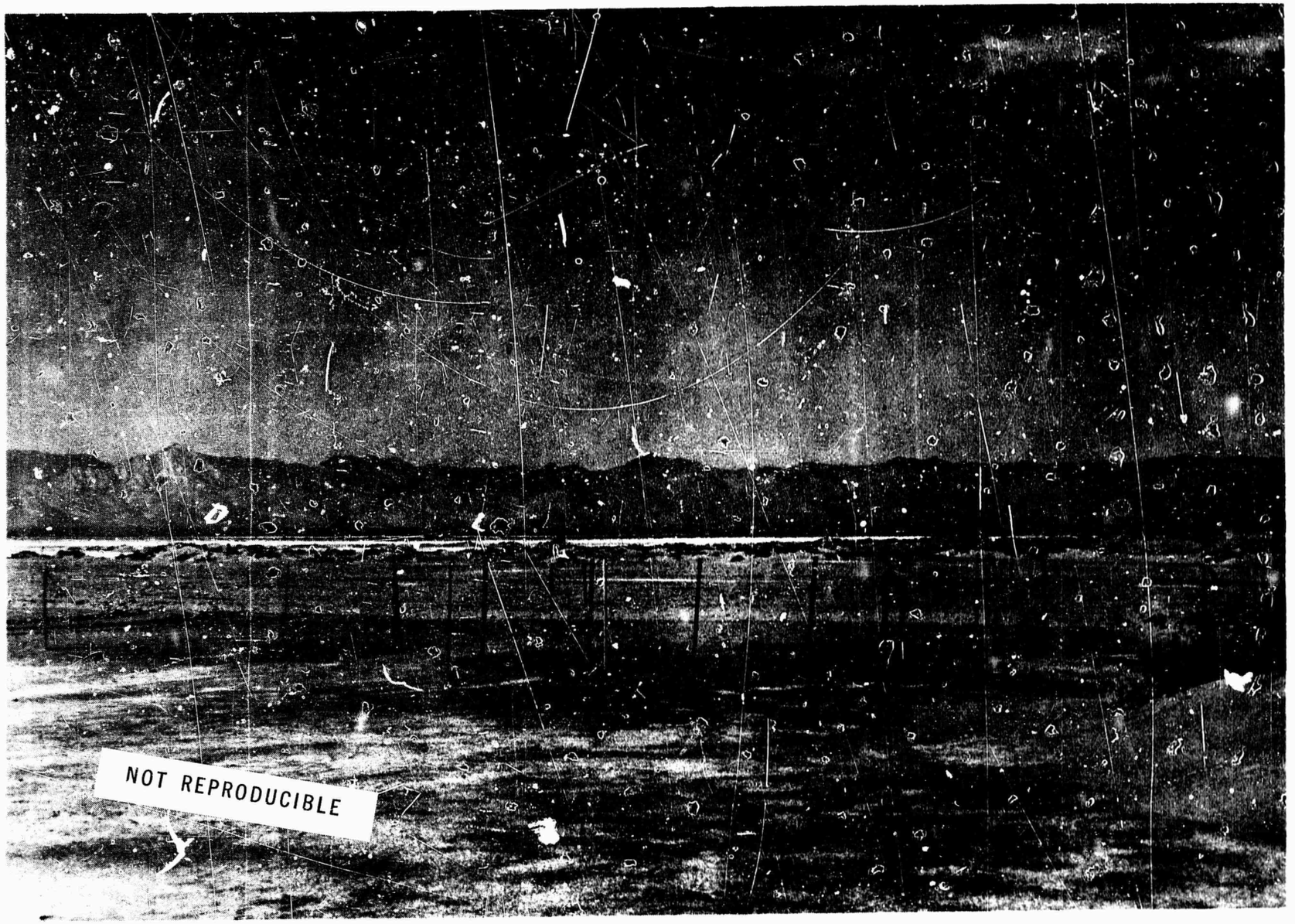

Figure 16 REPRESENTATIVE FRAGMENT DISTRIBUTION DATA (SIDE SECTOR F, CELL 4) FROM 15 BOMB STACK

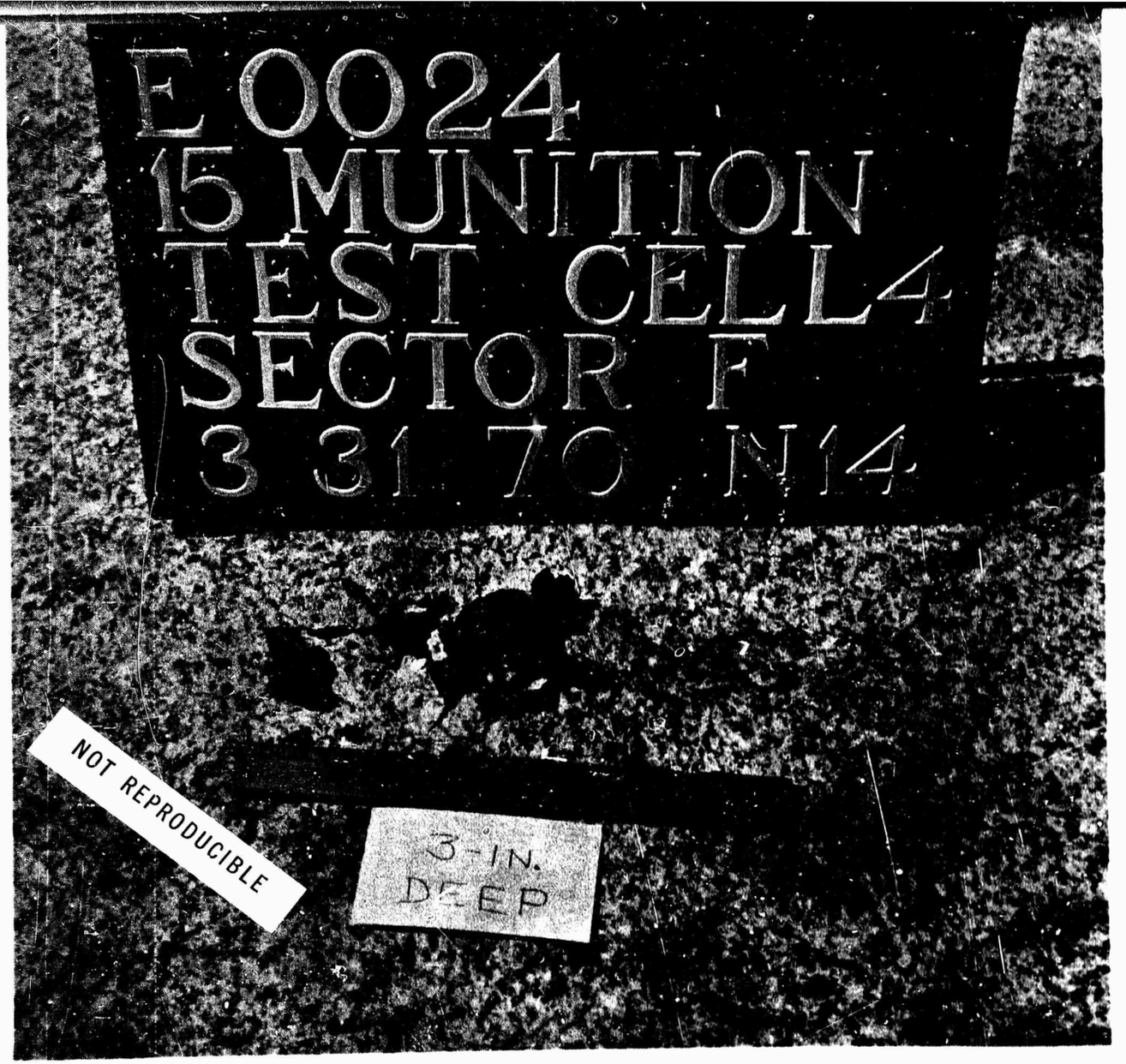

Figure 17 REPRESENTATIVE FRAGMENT IMPACT DATA (SIDE SECTOR F, CELL 4) FROM 15-BOMB STACK

Figure 18 REPRESENTATIVE FRAGMENT SIZE DATA (SIDE SECTOR F, CELL 4) FROM 15 BOMB STACK

from the sample cell; (b) the stakes mark the impact point of each fragment in the cell; (c) a typical fragment is shown embedded 3 in. in the hard-packed lake bed terrain; and (d) the relative size of fragment is illustrated. These collective data provide an illustration of the relative sizes and distributions of side-spray fragments at ranges from 500 to 2000 ft, as well as qualitative energy content of selected fragments. It was observed that the average fragment mass increased as the sample collection cell distance increased from the bomb stack.

The explosion crater sizes were measured for the two M117 bomb stack experiments. The pertinent crater data are tabulated in Table 4. A photograph of the six-bomb stack crater is shown as Figure 19, which illustrates the terrain that is typical for the dry China Lake test site.

TABLE 4
CRATER DATA

Crater Measurement	Six-Bomb Stack	15-Bomb Stack
Crest-to-Crest Diameter (ft)	29	45
Crest-to-Bottom Depth (ft)	10	14.4
Crest-to-Ground Height (ft)	2	3.7
Ground-to-Bottom Depth (ft)	8	10.7

4.4 Bomb Fragment Data Reduction and Presentation of Results

To assure that meaningful data were obtained from the two M117 bomb stack experiments, IITRI assumed the responsibility of processing the collected fragments. The fragment processing method that was utilized had previously been employed successfully in fragment performance tests under Contract F08635-67-C-0056 (IITRI Project B6077).

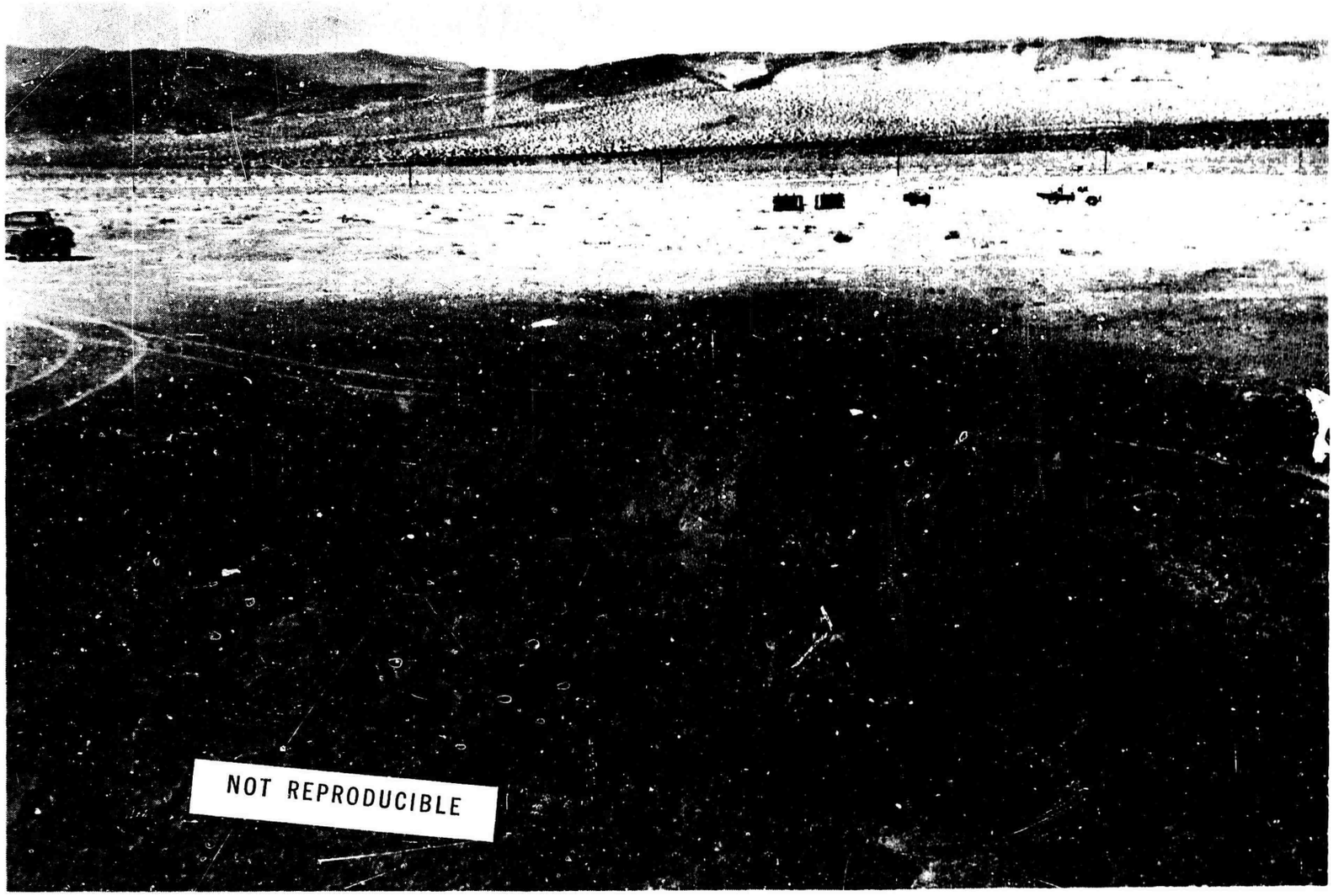

Figure 19 CRATER FOR SIX-BOMB STACK DETONATION

Upon receiving the fragments from NWC, the total fragment weight in each of 64 collection cells was weighed for the two-bomb stack experiments. These data are tabulated in Tables 5 and 6, with explanatory notations. Several observations were made concerning the fragment distribution from the stacked bomb experiments.

- The symmetrically located collection sectors (AG, BR, CE) yielded similar total weight values which indicated simultaneous bomb stack detonation was achieved.

- The total fragment weight distribution in the collection sectors appeared to be proportional to the unmasked bomb case metal facing the given sector. The side-spray sectors (B&F) yielded the highest total weights for the six bomb stack, while the nose and base sectors (D&H) were high for the 15 bomb stack. The nose ogive of the bombs contributed significantly to the total weight collected in sectors (C&E) located 45 degrees apart from nose sector D. Sectors (A&G) located 45 degrees apart from base sector H had the lowest total weights and the lowest bomb case mass facing the sectors.

- Cell 1 of base sector H had the highest total weight among the sector cells for both experiments. The total weights of all other sectors were converging about 1,900 to 2,000 ft distances (cells 2 and 1). These data indicated that the highest energy fragments may have been projected beyond the 2,000 ft range of sector H.

Based upon these observations, the fragment samples collected from cells symmetrically located with respect to the nose-to-base axis of the stacks were combined. The combining of symmetrical fragment cells enhanced the statistical sample size for determining fragment characteristics. In this manner, 40 distinct samples were obtained from the original 64 cells in each experiment.

The 40 fragment samples were processed in accordance with the following procedure.

- The fragment sample was screened on metallurgical sieves which separated the fragments into 12 size intervals.

TABLE 5

TOTAL FRAGMENT WEIGHT (lbs) IN EACH CELL FOR SIX BOMB STACK

Cell No.	A	B (Side)	C	D (Nose)	E	F (Side)	G	H (Base)	Total Wt. in Cells
1	1.08	1.85	2.32	0.18	2.32(1)	1.71	0.68	5.21	15.35
2	0.74	3.70	2.65	1.12	2.65(1)	3.90	0.54	3.95	19.25
3	1.40	2.78	2.90	1.87	2.47	5.45	0.60	2.00	19.47
4	0.58	5.32	1.63	1.78	1.63(1)	5.60	1.11	1.72	19.37
5	0.99	3.99	1.48	1.44	1.90	3.77	0.80	2.12	16.49
6	1.76	3.94	1.30	2.70	1.85	4.00(2)	0.67	2.00	18.22
7	0	2.13	1.95	1.42	1.03	3.82(2)	0.83	2.09	13.27
8	0.03	2.06	1.44	1.75	0.79	1.86	0.85	1.78	10.56
1-8	6.58	25.77	15.67	12.26	14.64	30.11	6.08	20.87	Sector Wts.

(1) These cells were unsuitable for fragment collection; symmetrical cell weights assumed.

(2) Approximately 50% collection due to wet terrain; actual collected weights were 200 and 1.91 lbs, respectively.

TABLE 6

TOTAL FRAGMENT WEIGHT (lbs) IN EACH CELL FOR 15 BOMB STACK

Cell No.	A	B (Side)	C	D (Nose)	E	F (Side)	G	H (Base)	Total Wt. in Cells
1	0.02	1.32	4.64	17.50	4.64(1)	0.91	1.32	23.63	53.98
2	1.40	8.47	6.43	26.05	6.43(1)	3.80	1.63	17.75	71.96
3	1.60	5.58	4.04	19.77	4.14	3.32	2.50	12.39	53.34
4	1.74	8.09	7.34	24.11	5.75	9.32	1.77	8.83	66.95
5	2.52	4.91	6.14	17.59	5.16	3.18	2.18	7.45	49.13
6	2.80	5.20	7.22	21.31	5.34	6.22(2)	2.04	11.15	61.28
7	1.86	3.83	5.05	13.83	5.63	4.16(2)	2.28	6.78	43.42
8	2.21	3.07	6.58	9.87	2.47	3.90	1.83	6.59	36.52
1-8	14.15	40.47	47.44	150.03	28.49	36.74	15.55	94.57	Sector Wts.

(1) These cells were unsuitable for fragment collection; symmetrical cell weights assumed.

(2) Approximately 50% collection due to wet terrain; actual collected weights were 3.11 and 1.91 lbs, respectively

- The total weight was obtained for each graded sample fraction.

- The number of fragments was counted in each graded sample fraction.

The most significant parameter associated with the fragment processing procedure is the proper selection of metallurgical sieves which determine the fragment mass categories. To obtain meaningful fragment hazard information, it was imperative that good resolution be provided for the larger fragments, as well as the smaller fragments related to the performance of the munition. Based upon this premise, a set of twelve sieves was selected ranging from 1 in. to No. 8 mesh sizes, which provided average fragment mass categories ranging from about 133.8 grams (2,000 grains) and 0.15 gram (2.4 grains), as shown on Tables 7 and 8 for the two M117 bomb stack experiments.

These data represent a summary of all bomb fragments retained by a given metallurgical sieve. It is significant to observe that more than 50 percent of the recovered fragment weight was screened out by the four largest mesh sizes, while the number of fragments retained represented only 3 to 6 percent of the total number counted. The average fragment weights for the two experiments were 6.0 and 3.3 grams, respectively.

An automated fragment counting apparatus was used to determine the number of fragments retained in each sieve. This IITRI-fabricated apparatus consists of a bowl feeder and trough arrangement which aligns the fragments and conveys them through the beams of a photoelectric counting device. From the number and weight of fragments retained on each sieve, the desired average mass for each graded sample fraction was calculated.

The IITRI fragment processing method has been compared with the computerized individual weighing and counting techniques employed at Picatinny Arsenal. The IITRI procedure was demonstrated to yield fragment distribution data identical to those obtained by the Picatinny method.

TABLE 7

SIEVE DATA FOR SIX-BOMB STACK EXPERIMENT

Sieve Mesh Size (in.)	Avg Frag. Wt (gm)	No. of Frag. in Given Sieves	Wt of Frag. in Given Sieves (gm)
1	133.8	129	17,259.3
7/8	67.4	94	6,340.5
3/4	41.8	129	5,395.1
5/8	26.4	228	6,028.4
1/2	14.2	440	6,271.3
7/16	8.0	359	2,868.8
3/8	4.9	604	2,979.3
5/16	3.0	706	2,137.6
1/4	1.8	1266	2,121.2
No. 4	0.80	2000	1,609.3
No. 6	0.33	2171	725.2
No. 8	0.15	953	140.0
< No. 8			805.0
	Totals:	9079	54,681.0

Average Fragment Weight: 6.0 grams

TABLE 8

SIEVE DATA FOR FIFTEEN-BOMB STACK

Sieve Mesh Size (in.)	Avg Frag. Wt (gm)	No. of Frag. in Given Sieves	Wt of Frag. in Given Sieves (gm)
1	146.0	363	52,992
7/8	61.7	228	14,070
3/4	39.2	479	18,787
5/8	23.5	886	20,841
1/2	12.9	1,824	23,490
7/16	7.9	1,619	12,804
3/8	5.2	2,348	12,142
5/16	3.0	2,934	8,699
1/4	1.6	5,352	8,854
No. 4	0.84	9,905	8,286
No. 6	0.34	16,728	5,607
No. 8	0.14	16,000	2,242
< No. 8			2,549
	Totals:	58,666	191,362

Average Fragment Weight: 3.3 grams

5. FULL-SCALE 155mm SHELL TESTS

The fragmentation data obtained from the M117 bomb stack experiments provided strong evidence that fragment distribution characteristics may be quite sensitive to the physical configuration of the munition. That is, the fragment hazards from stacked artillery projectiles may differ significantly from stacked aerial bombs because of the differences in the metal case configuration and the explosive charge-to-metal mass ratio.

To obtain additional data concerning the role of munition configuration in the fragment hazard study, IITRI requested permission through the ASESB, to participate in two 155mm projectile stack experiments that had been planned previously at the Yuma Proving Ground by the Army Materiel Command (AMC). Communications with the AMC-Yuma test director indicated that the first experiment consisting of 1000 units of 155mm projectiles stacked 10 high and 100 wide to be detonated in open store would provide an excellent source to obtain fragment hazard data. Furthermore, it was established that a modified IITRI fragment collection network could be superimposed on the AMC-Yuma experiment without interference to the primary test objectives.

5.1 Description of AMC-Yuma Experiments

The AMC-Yuma experiments used two configurations of stacked 155mm shells as shown in Figure 20. The first experiment consisted of 1000 units of 155mm shells stacked 10 high and 100 wide in a parallel array with minimum spacing between projectiles. The stack was detonated by a single, centrally located 155mm projectile with the remainder of the stack initiated by sympathetic detonation.

The second experiment consisted of three stacks of 1000 155mm projectiles each, 10 projectiles high by 100 projectiles long. The center, or donor, stack was oriented nose-to-nose with respect to one and base-to-base with respect to the other. The stacks were 50 in. apart.

The primary objectives of the AMC program plan may be outlined as:

A. Yuma 1000 Unit 155mm Projectile Stack Test

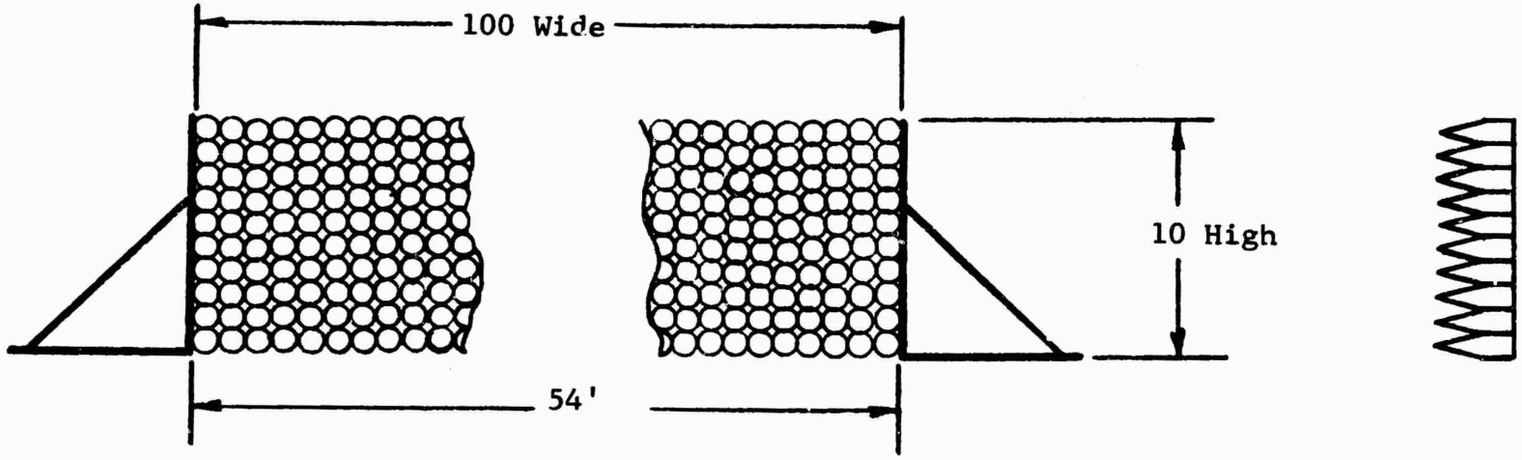

B. Yuma 3000 Unit 155mm Projectile Stacks Test

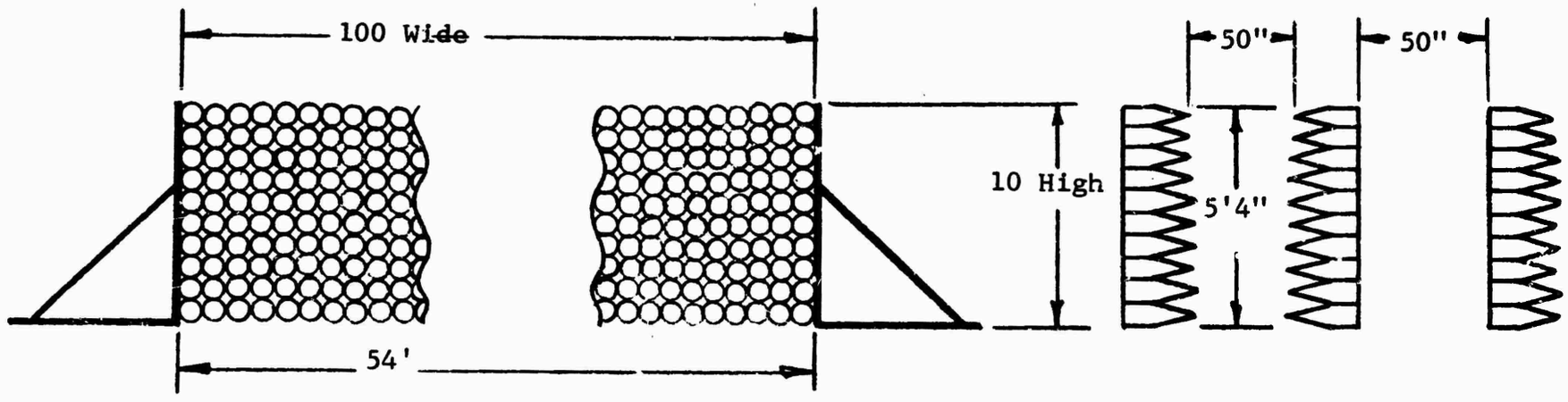

Figure 20 YUMA PROVING GROUND 155mm PROJECTILE STACK TESTS

- Obtain blast pressure measurements at gage stations located from ground zero to 2200 ft distances along gage lines direct from the nose, base and side orientations from the munition stack.

- Obtain photographic data on explosion propagation and fragment velocity from steel witness panels (8 ft x 24 ft x 1/8 in. thick) located about 250 ft from nose of stack.

- Obtain fragment recovery and penetration data from Celotex collection units (8 ft x 88 ft x 4 ft thick) about 250 ft from noses of stock.

- Obtain ion probe data for detonation propagation velocity along length of stack.

The IITRI fragment recovery program represented a secondary objective of the experiment which was designed to obtain farfield fragment data without any interference with the basic plans.

The IITRI activity in the Yuma experiments was designed to investigate the role of the 155mm shell configuration in determining fragment hazard characteristics of these stacked projectiles in open store. By analyses of recovered farfield fragments, meaningful information was expected concerning fragmentation characteristics of these stacked projectiles, and fragment density at various distances and orientations from the stack.

The 155mm artillery projectiles used in these experiments incorporated these nominal parameters of interest:

- Total assembly weight: 90 lbs
- Composition B explosive weight: 15 lbs
- Metal component weight: 75 lbs

The projectiles were provided with ring-type nose plugs and protective grommets on the rotating bands. The stacked projectiles were supported by wooden end structures, and plywood shim dunnage; only as required to maintain stack levelness. Thus all recovered fragments were components of the projectile case material.

5.2 Fragment Collection Procedure

A month prior to the scheduled test data, the Yuma Proving Ground test site was inspected, and detailed IITRI-Yuma program specifications were modified to accommodate practical considerations. It was determined that the IITRI eight-sector fragment collection network (used successfully at NWC-China Lake) would result in prohibitively high preparation costs due to the relatively rugged Yuma terrain. The solution was to exploit preparation requirements for the AMC-Yuma pressure-gage stations which extended 2200 ft radial distance from the projectile stack. The modified version of the IITRI fragment collection network was made to correspond to the three gage-line orientations directed from the nose, base and side-spray azimuths of the munition stack. The fragment collection sectors and gage-line installations complemented each other by mutually requiring clear and level terrain to obtain meaningful data output, as well as sharing basic orientation requirements. In addition, the three sectors reduced the anticipated fragment collection weight to a manageable level; to provide a minimum cost approach with no compromise in obtaining the essential fragment hazard information.

Although three full-size fragment collection sectors were prepared prior to the experiments, the unexpected fragment distribution characteristics from the 155mm projectile stack resulted in decisions to modify the three collection zones as illustrated on Figure 21. Side-spray sector C was retained as a full-size zone, but is shown displaced by 15 degrees, to take advantage of the existing level terrain. Nose sector A was reduced 50 percent in an area by lowering the sector angle from 8 degrees 36 min to 4 degrees 18 min. Finally, base sector B was reduced to a fragment collection strip 50 ft wide extending from 500 to 2000 ft radial distance from the stack. All three collection sectors retained the eight-cell division to maintain consistent farfield distances. Although each cell differed in area, the

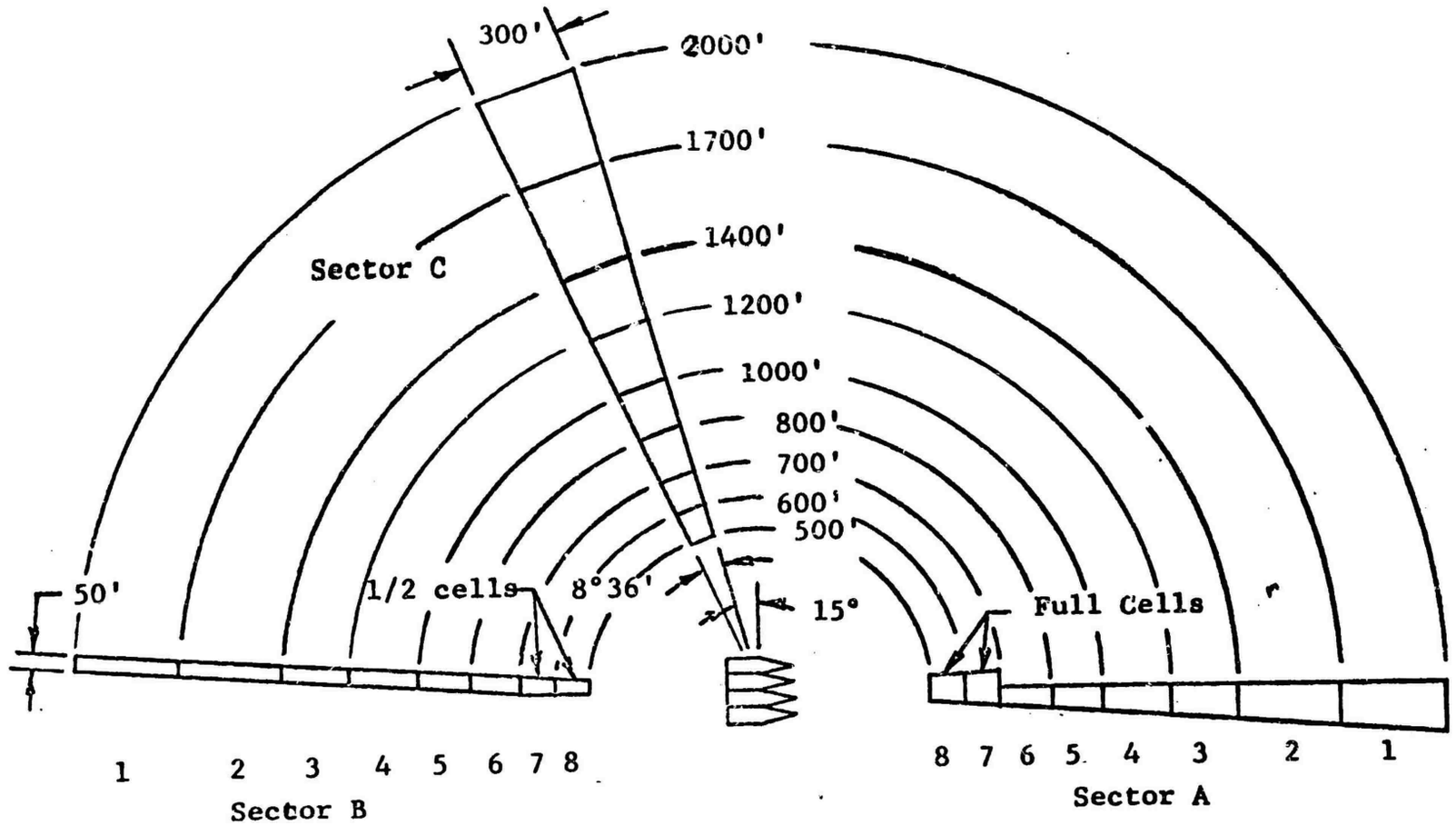

Figure 21 YUMA FRAGMENT COLLECTION CELL SPECIFICATIONS

fragment weights collected in the cells represented significant statistical samples suitable for normalized fragment distribution data.

To assure consistent fragment collection data, the truck-mounted electromagnet used in the M117 bomb stack experiments was procured from NWC-China Lake, as well as NWC operating personnel. The proven collection procedure established during the NWC bomb stack experiments was used as described in Section 4.2 of this report. All collected fragment samples were deposited in properly identified containers and shipped to IITRI for fragment data analyses.

5.3 Analysis of Yuma Experimental Results

The first experiment consisting of a single, 1000-unit, 155mm projectile stack yielded farfield fragment distributions radically different from that associated with the detonation of a single munition. An inspection of nose sector A confirmed the expected heavy concentration of nose-end fragments along the total collection zone. However, an examination of the side-spray sector C and a large region adjacent to the surveyed zone, revealed that a relatively insignificant number of fragments were available. An unexpected explanation was found in base sector B wherein an unexpectedly high fragment density was present throughout the collection zone. Upon closer inspection, sector B was laden with projectile side-wall fragments of relatively massive proportions, i.e., 9 to 18 in. long by 4 to 6 in. wide weighing in excess of 5 lbs, as well as the expected base fragments.

The second Yuma experiment verified the anticipated detonation characteristics of the projectile stacks. As predicted, only the donor stack detonated, while the adjacent acceptor stacks were projected as intact projectiles up to 4500 ft distances from ground zero. The acceptor stacks did provide some measure of masking of donor stack fragments projected from the nose and base orientations. This was evidenced by a substantial increase in the mass of fragments remaining at ground zero. Careful inspection of base sector B revealed a marked reduction in the number of massive side-wall fragments distributed in the cleared zone. Both base

sector B and nose sector A showed a substantial decrease in fragment density beyond about 1400 ft. However, side sector C maintained its unexpectedly low fragment density.

A comparison of the total recovered fragment weights for each cell from the two Yuma experiments is shown on Table 9. These data provide firm evidence that the acceptor stacks blocked a significant number of the longer ranged fragments (cells 1 and 2) in the nose and base sectors, while the side-spray fragment distribution remained essentially the same for both experiments. It should be emphasized that the total weight data shown in Table 9 were obtained from three sectors which differed significantly in size, (see Figure 21).

A relative measure of the fragment weight density for the three sector orientations was obtained by calculating the fragment weight as a function of equivalent collection areas. These data for the two experiments are summarized in Table 10. Based upon equivalent area comparisons, the base sector B fragment weight was more than twice as great as that for nose sector A, and more than 20 times that for side sector C. In addition, a comparison of the weight ratios from the two experiments provide some estimate of the fragment mass that was blocked by the acceptor stacks in the second experiment.

The presence of massive concentrations of projectile side-wall fragments in base sector B represented a major complication that must be resolved in terms of initial fragment field input for an analytical stack model. It may be theorized that the 155mm shells in the environment of a sympathetically detonated stack may have a mechanism of fragmentation analogous to peeling a banana. The resultant massive side-wall fragments are a radical departure from the fragmentation distribution associated with the detonation of a single 155mm projectile in both orientation and mass categories. These data verified that the physical configuration and the explosive charge-to-metal mass ratio of the munition plays a significant role in the assessment of fragment hazards associated with stacked munitions in open stores.

TABLE 9

YUMA EXPERIMENTS: COMPARATIVE RECOVERED FRAGMENT WEIGHTS (lbs)

Collection Cell Number	Nose Sector A		Base Sector B		Side Sector C	
	1st Test	2nd Test	1st Test	2nd Test	1st Test	2nd Test
1	88.8	71	165.6	64	17.0	17
2	97.2	172	333.9	162	30.2	38
3	281.2	173	259.3	305	(46.0)	46
4	237.3	259	359.0	375	38.2	51
5	278.9	287	261.4	340	44.3	39
6	428.1	275	280.4	378	44.4	45
7	268.4	303	272.5	270	43.3	42
8	229.5	184	186.1	167	45.1	85
Totals	1909.4	1724	2118.8	2061	308.5	363

1. Side sector C, cell 3 of first test was lost; weight data from second test is listed to provide total weight balance.

2. Refer to Figure 1 to obtain fragment collection cell specifications.

TABLE 10

YUMA EXPERIMENTS: NORMALIZED FRAGMENT WEIGHT DATA

Sector Orientation	Collection Area (ft^2)	Area Factor	Recovered Frag. Wt. (lbs)	Normalized[1] Frag. Wt. (lbs)	Weight[2] Ratio
	1st Test: One Row, 1000 unit, 155mm Shell Stack				
A-Nose	140,625	2	1909.4	3,818.8	12.4
B-Nose	75,000	3.75	2118.8	7,945.5	28.8
C-Side	281,250	1	308.5	308.5	1
	2nd Test: Three Rows, 1000 unit, 155mm Shell Stack				
A-Nose	140,625	2	1724	3,448	9.5
B-Base	75,000	3.75	2061	7,729	21.3
C-Side	281,250	1	363	363	1

1. Normalized fragment weights reflect sector fragment mass associated with full-size IITRI collection area, e.g., side sector C.
2. Weight ratio indicates comparison with recovered weight of sector C.

6. ANALYTIC-EXPERIMENTAL COMPARISONS

This section attempts to show the feasibility of applying the results of the small-scale munition stack experiments to existing single bomb initial field fragmentation data. Here, farfield data, utilizing the analytic trajectory model obtained in Phase II, is computed and compared to data collected at NWC, China Lake for each of two munition stack configurations. While these comparisons are by no means exact, there are not order-of-magnitude differences at comparable ranges and zones.

From the set of small-scale and full-scale experiments which were run several general observations qualifying results obtained can be made. These include:

(1) The small-scale tests indicate discrete zones of material enhancement which is dependent on stack configuration and spacing. Since the small-scale tests were conducted with cylinders, this effect is only valid for the side-spray direction.

(2) The full-scale bomb tests at China Lake have shown that the fragment input data, obtained for a single munition, lacks adequate resolution for the heavier fragment weights.

(3) The Yuma tests indicate that the fragment size may vary as a function of individual munition case design, stack configuration, and mode of initiation.

Since the Yuma results have exhibited rather unexpected phenomena which are at present not fully understood, the present discussion will be limited to the techniques now being employed to analytically simulate the M117 bomb test results, obtained at China Lake.

6.1 Modified Initial Fragment Field Data

In the Fragmentation Hazard Study, Phase II, test results for single munitions were utilized as input to an analytic model which mapped initial fragment field data into the farfield. These test results defined the initial spatial field of fragment masses, velocities and elevation angles. The full-scale bomb test results from China Lake have shown a predominance of heavy fragments in the farfield. The input data, available from Eglin Air Force Base, on the other hand, groups heavier fragments into only two mass categories. It was therefore necessary to modify the input data into a more meaningful mass distribution.

Available data give an average weight and total number of fragments for a given weight class in a given polar angle. The Eglin data gave a good distribution up to and including weight classes below 463 grains. All fragments in excess of this weight were lumped into one fragment class and defined by an average fragment weight and the total number of fragments recovered in each of the polar sectors. Also given was the weight of the largest fragment found in each polar sector.

A new distribution was defined using the total weight in the top mass category, the total amount of fragments in this category and the largest fragment found in a polar zone. For a given polar zone the new distribution was defined by picking one fragment corresponding to the largest in that polar zone and arbitrarily picking fragments between that largest size and 463 grains. Although the method was arbitrary the number of fragments and the total weight was conserved. Figure 22 shows how the final distribution looks when percent of accumulative weight is plotted as a function of fragment weight. Portion A of the curve represents the Eglin data up to 463 grains while portion B is the modified data giving finer resolutions at the higher weight categories.

6.2 Stack Model Adjustments to Input Data

In order to adjust the initial field data for one munition to reflect the enhancement rules developed from the set of small-scale experiments, Figure 7 was utilized to obtain amplification factors at appropriate elevation angles. Before going any further in the discussion it is appropriate to define the initial fragment source geometry.

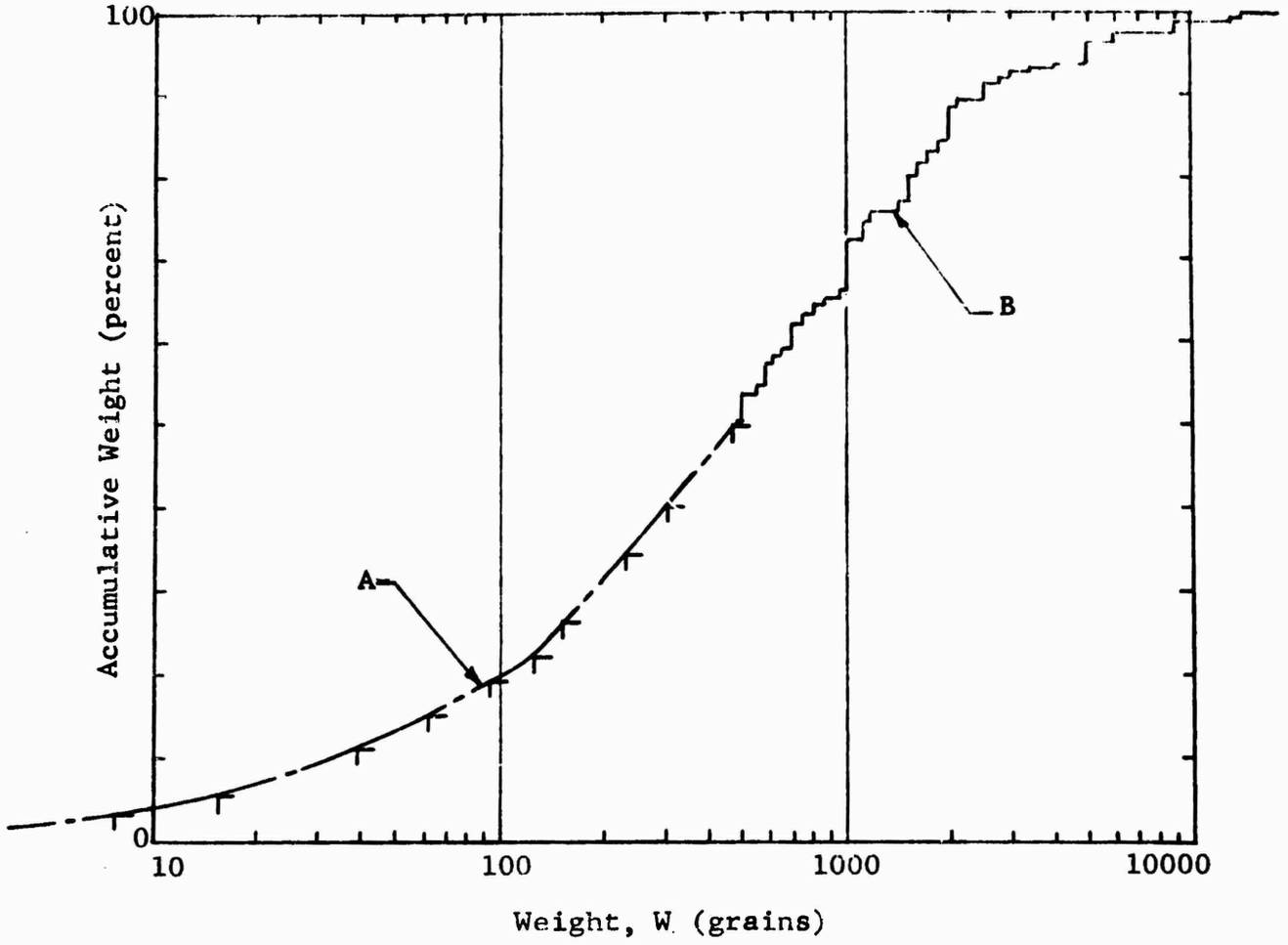

Figure 22 ACCUMULATIVE WEIGHT FOR SINGLE BOMB

TABLE 11

TYPICAL FORMAT OF EXPERIMENTAL DATA FOR MUNITION OF INTEREST

Mass Intervals (grains) / Polar Zone (degrees)	o - m_1		m_1 - m_2		. . . .	m_8 - m_9		Above m_9		Total Number of Fragments	Initial Velocity
	W_{AV}	$\bar{N}$	W_{AV}	$\bar{N}$		W_{AV}	$\bar{N}$	W_{AV}	$\bar{N}$		
0 - 5	-	-	-	-	. . . .	-	-	-	-	-	-
5 - 10	-	-	-	-	. . . .	-	-	-	-	-	-
10 - 15	-	-	-	-	. . . .	-	-	-	-	-	-
.	.	.	.	.	. . . .	.	.	.	.	.	.
.	.	.	.	.	. . . .	.	.	.	.	.	.
.	.	.	.	.	. . . .	.	.	.	.	.	.
.	.	.	.	.	. . . .	.	.	.	.	.	.
170 - 175	-	-	-	-	. . . .	-	-	-	-	-	-
175 - 180	-	-	-	-	. . . .	-	-	-	-	-	-

Where: W_{AV} is average weight, $\bar{N}$ is average number of fragments.

The fragments from a munition considered as a point source on the ground may be regarded as originating from positions on a hemispherical envelope enclosing the source. Each point of origin on the hemisphere defines an elevation angle α_o and an azimuth ϕ in the horizontal plane measured from the nose of the munition. Figure 23 defines these two angles with respect to the fragment geometry.

The format of typical munition data is shown in Table 11. Fragments in all mass intervals are assumed to be emitted from a given polar zone at the same velocity. This table will be modified by applying appropriate weighting factors to the data as a function of elevation angle and azimuth. From Figure 7 the following amplification factors are given as a function of elevation angle in Table 12:

TABLE 12

AMPLIFICATION FACTORS

Test Configuration	Elevation Angle (Degrees)	Amplification Factor
3 x 2	0-11.25	5.75
	11.25-22.5	2.
	22.5 -67.5	1.
	67.5 -79.	1.5
	79. -90.	3.
3 x 5	0-11.5	5.75
	11.5-22.5	2.
	22.5-67.5	1.
	67.5-79	2.
	79. -90	10.5

6.3 Discussion of Comparative Results

Before going into a comparison of the China Lake test and analytic results a brief discussion concerning the sensitivity of the analytic results is needed.

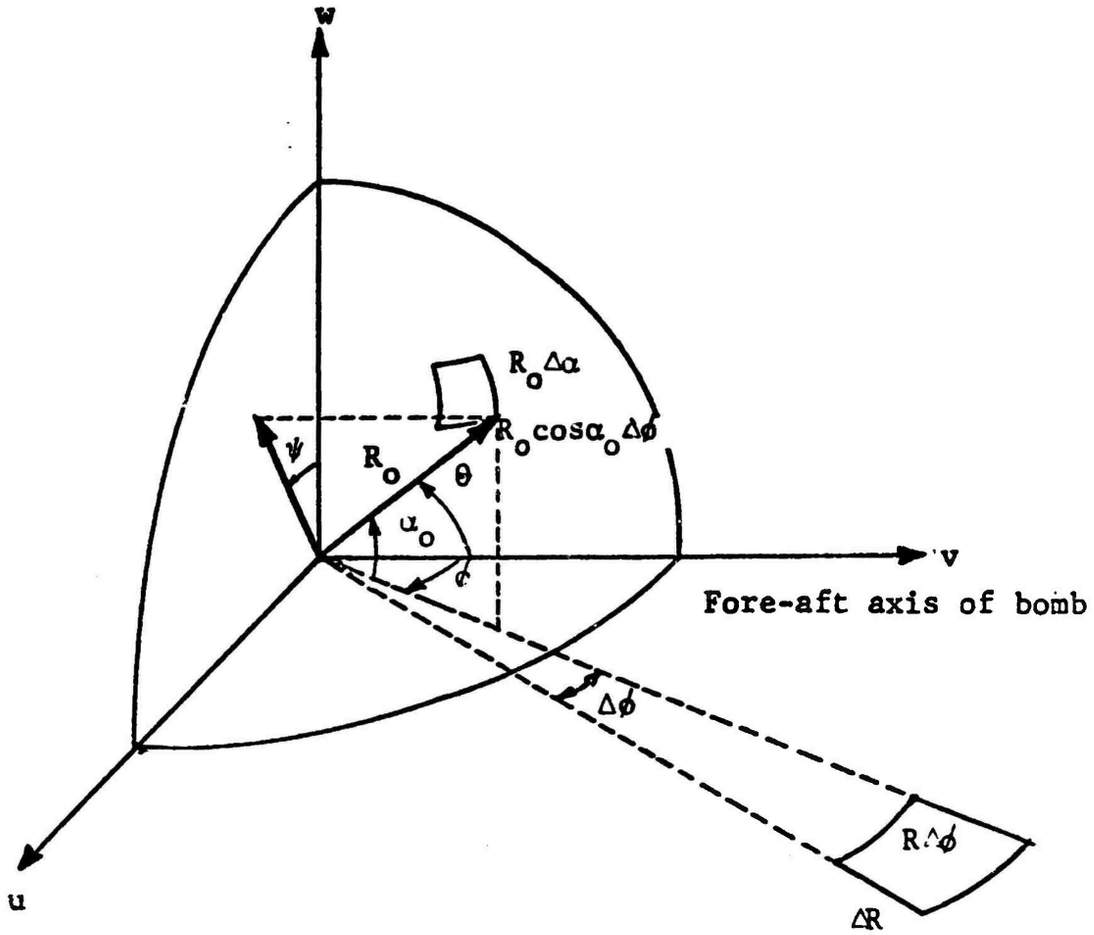

Figure 23 FRAGMENT SOURCE GEOMETRY

Figures 24 and 25 give trajectory characteristics of bomb fragments with high and low initial velocities. The scaled size of the collection zones, utilized in the China Lake tests have been superimposed here for reference. Within the collection zone (i.e., 2000 ft) the trajectory characteristics are not too sensitive to initial velocity. If the data, however, is presented as illustrated in Figures 26 and 27 the performance of the collection cells can be evaluated for light and heavy fragments. Figure 26 indicates that heavier fragments tend to be more abundant at the furthest collection zones (i.e., zones 4 to 1) while very few fragments should be collected in the closer zones. Fragments found in zones 5 through 8 correspond to very high elevation angle while fragments found in zones 4 to 1 are from lower elevation angles and from extremely low elevation angles. Figure 27 indicates a much more efficient collection performance for the light fragment. Here all fragments are concentrated within cells 8 to 4 and results for cells 8 to 5 would tend to be better than those for cells 1 to 4.

Figures 28 through 31 present the experimental-analytic comparative results for the two NWC bomb tests at China Lake in the 85 to 95 degree azimuth. This corresponds to the side-spray sector. Number densities are presented for a small mass category (i.e., 24.227 grains) and the total for all mass categories. These densities are presented in each of eight cells corresponding to collection zones ranging from 550 ft to 1850 ft from ground zero (i.e., the centroids of the experimental collection cells).

The results indicate that the low mass category fragments tend to have reasonably comparable density values within zones 5 through 8 (i.e., up to 900 ft). The overall results, which are dependent on the modified mass distribution and tend to be representative of heavier fragments, are comparable in zones 1 through 4 (i.e., beyond 900 ft). Agreement of the computed and experimental results within an order of magnitude is considered here to be an acceptable comparison. The above discussion pertains to both the six and 15 bomb results which should be relatively comparable in the side-spray azimuth as shown in Table 13.

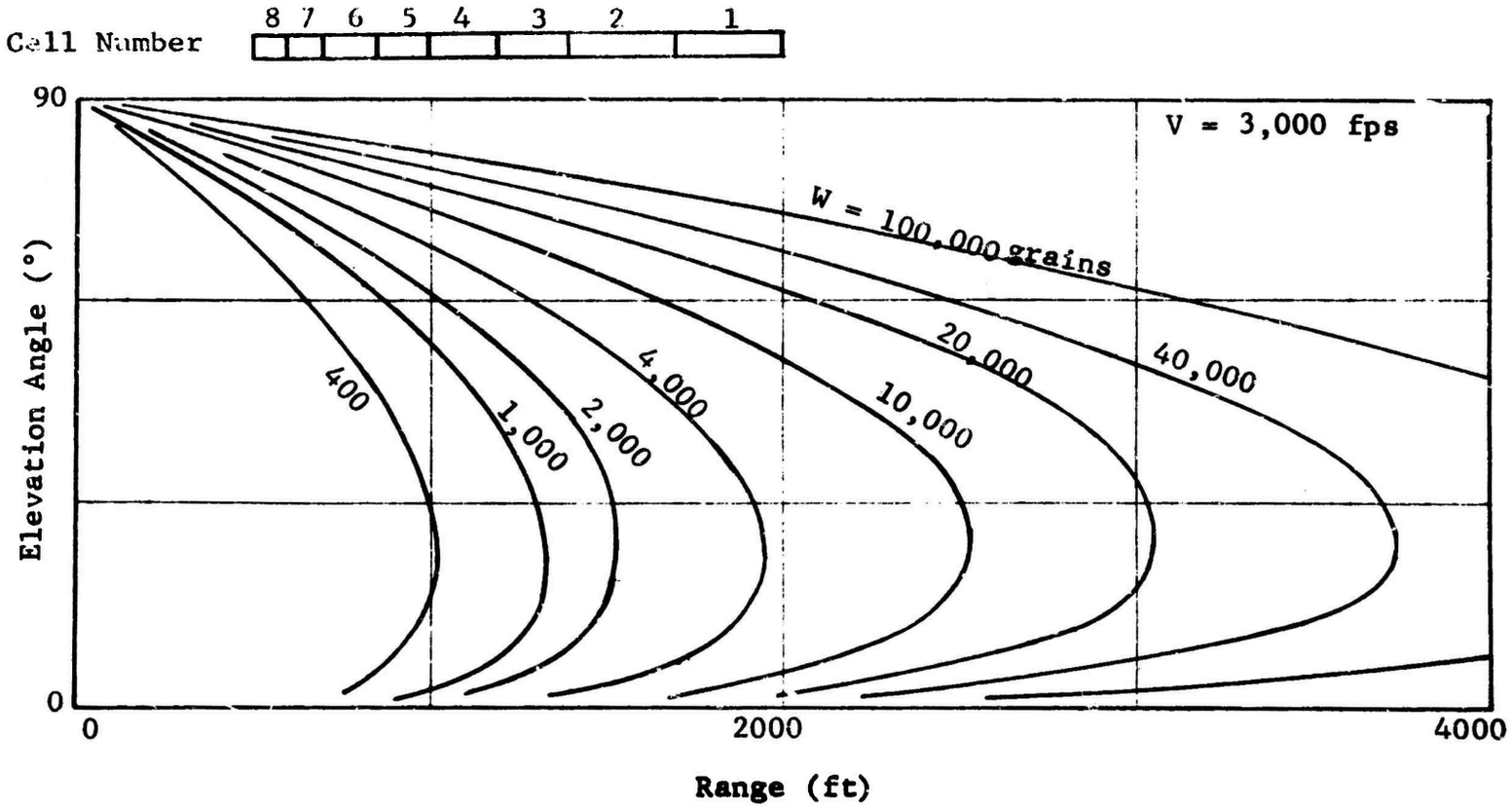

Figure 24 TRAJECTORY CHARACTERISTICS OF BOMB FRAGMENTS WITH AN INITIAL VELOCITY OF 3000 fps

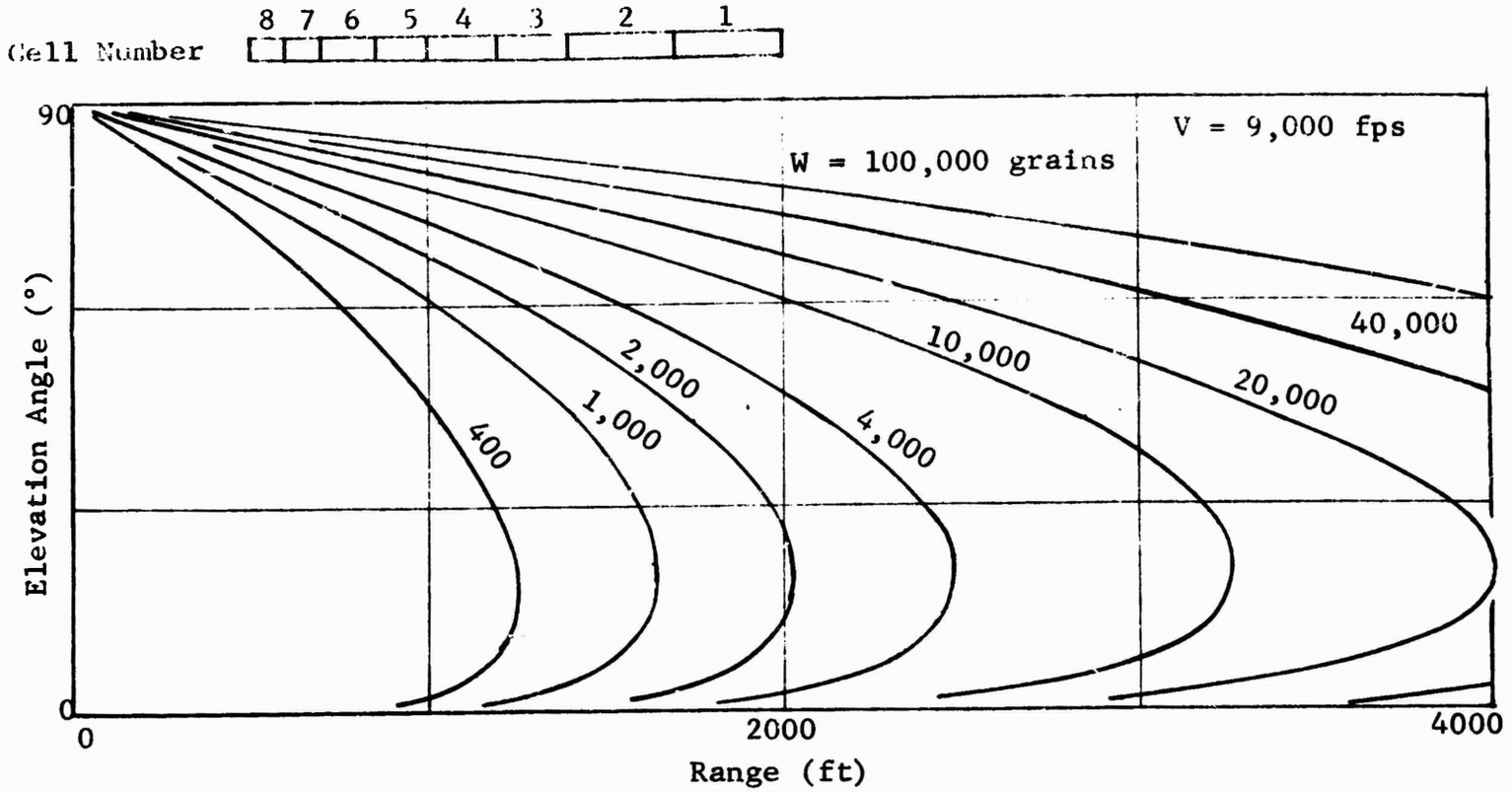

Figure 25 TRAJECTORY CHARACTERISTICS OF BOMB FRAGMENTS WITH AN INITIAL VELOCITY OF 9000 fps

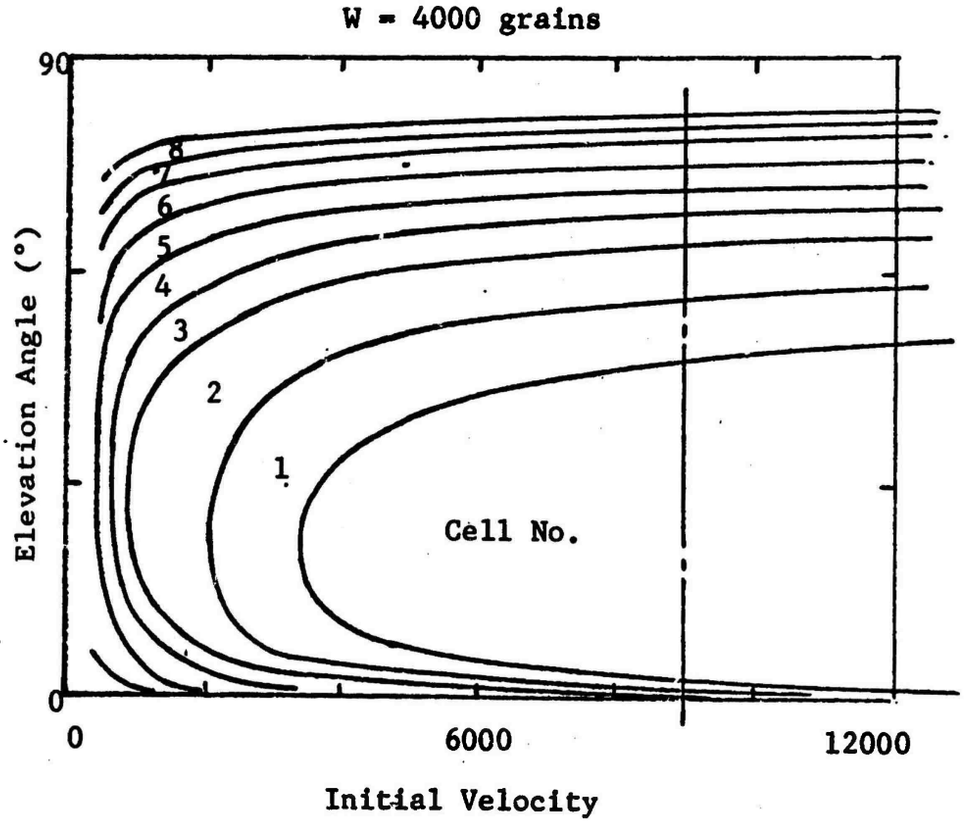

Figure 26 COLLECTION PERFORMANCE OF COLLECTION CELLS FOR 4000 GRAIN FRAGMENTS

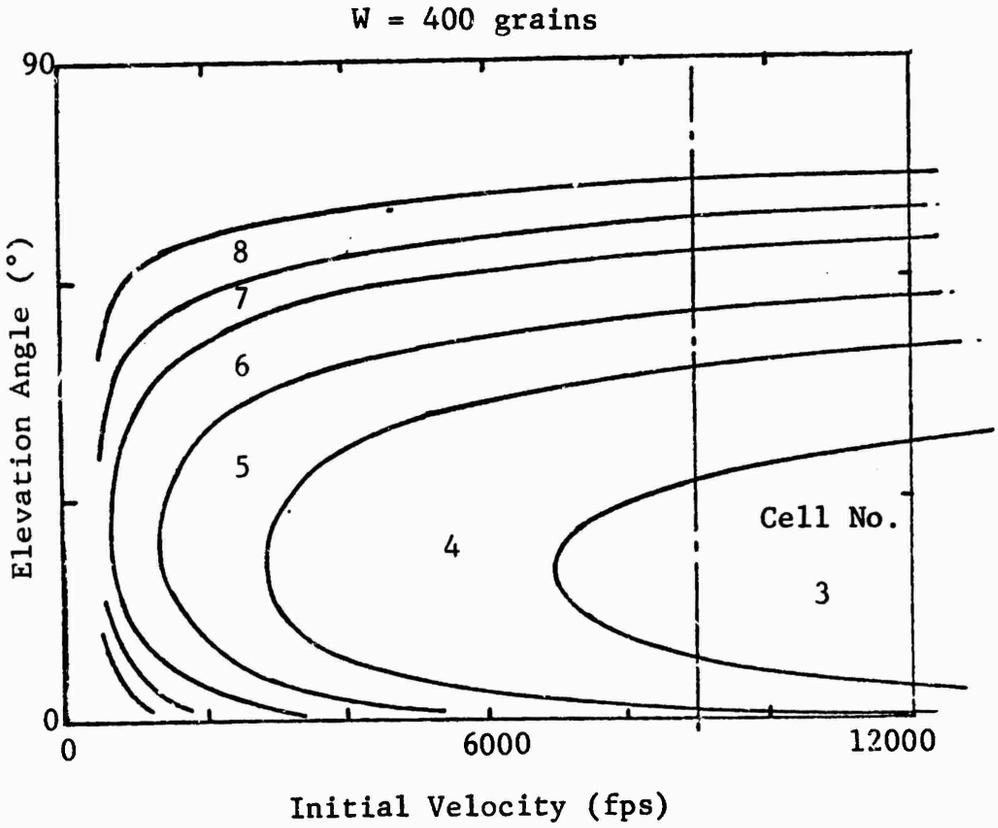

Figure 27 COLLECTION PERFORMANCE OF COLLECTION CELLS FOR 400 GRAIN FRAGMENTS

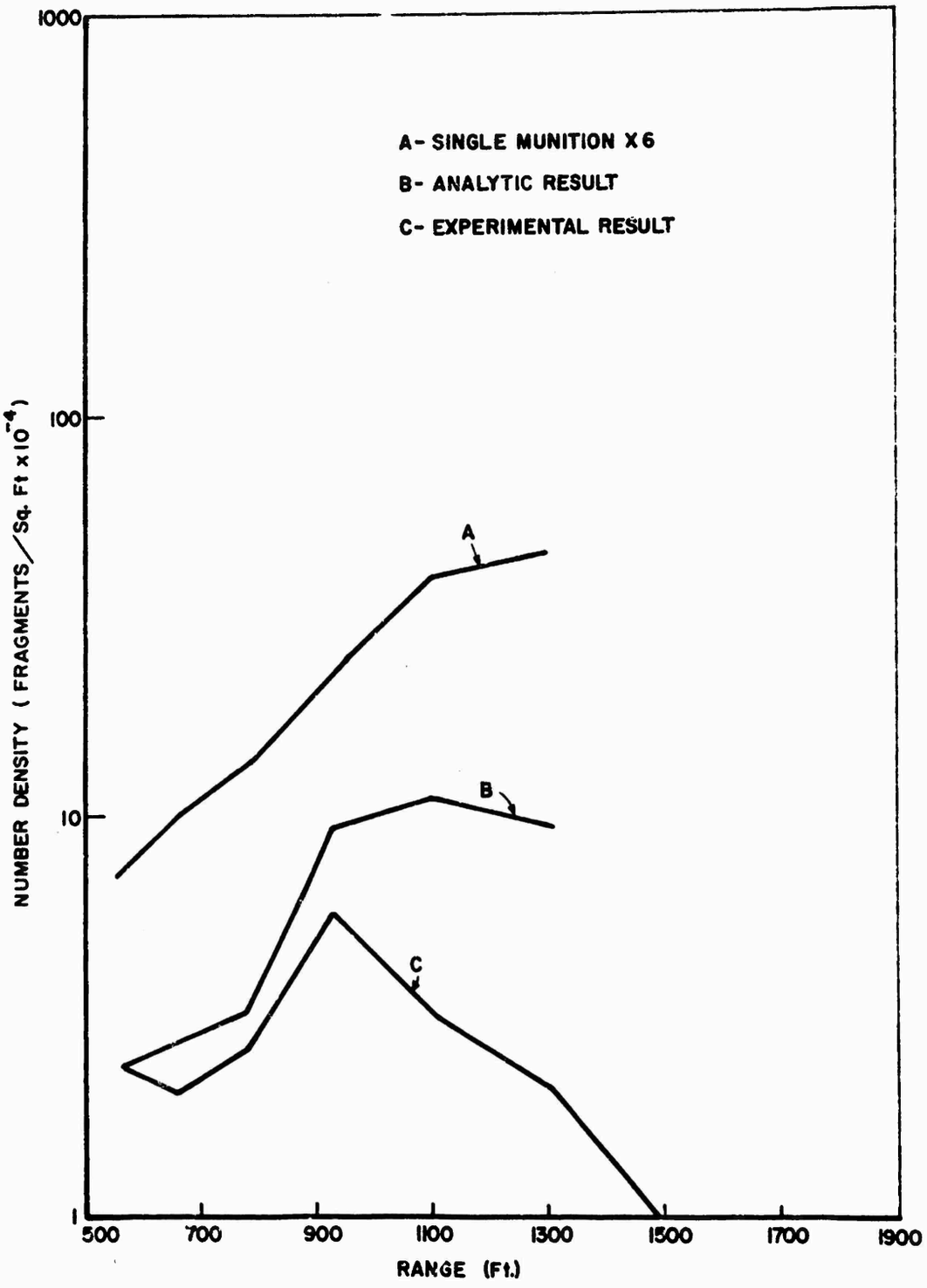

Figure 28 2x3 ANALYTIC-EXPERIMENTAL COMPARISONS FOR SMALL FRAGMENTS (MASS = 24.2 GRAMS)

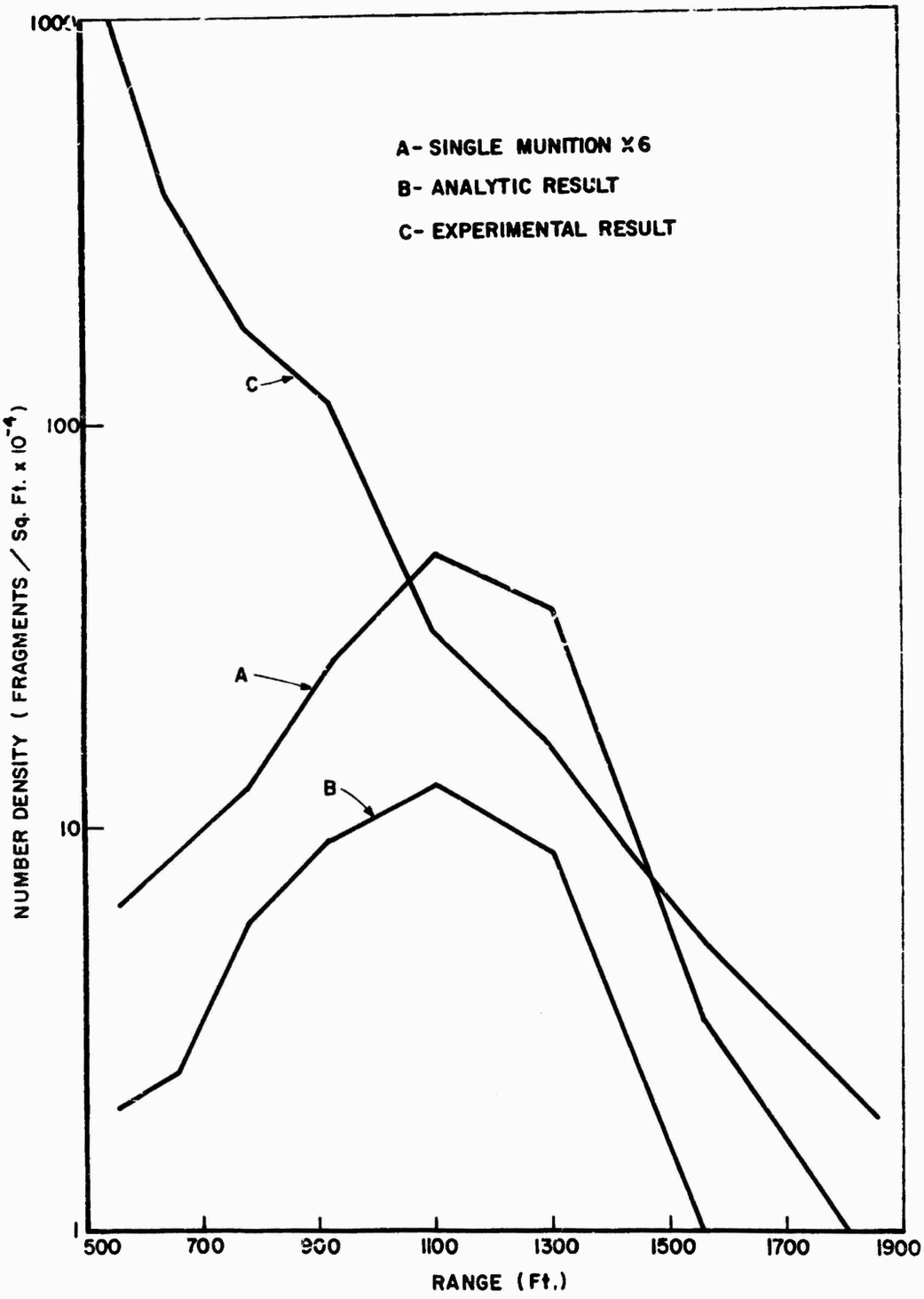

Figure 29 2x3 ANALYTIC-EXPERIMENTAL COMPARISONS FOR ALL FRAGMENTS

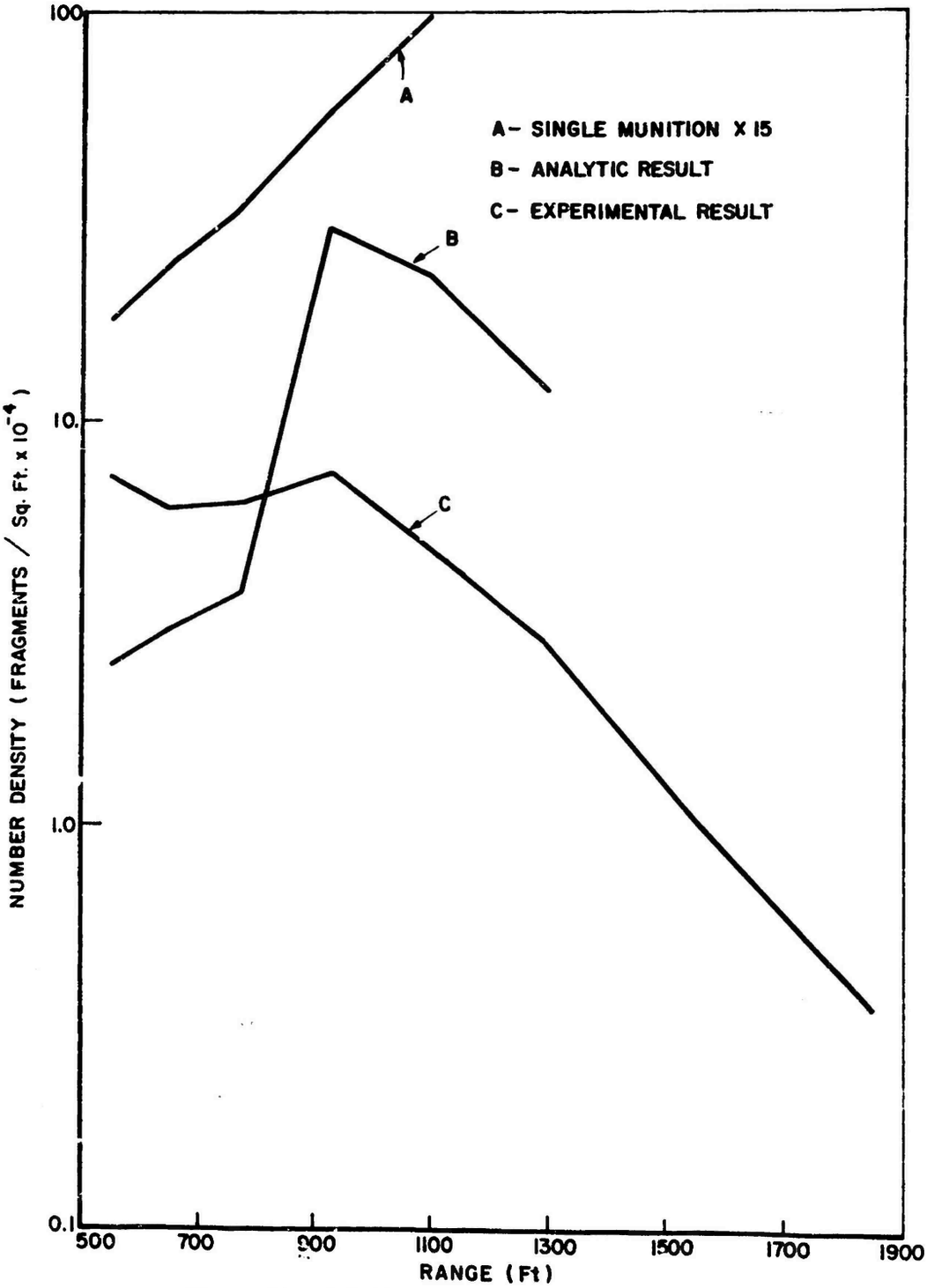

Figure 30 3x5 ANALYTIC-EXPERIMENTAL COMPARISONS FOR SMALL FRAGMENTS (MASS = 24.2 GRAMS)

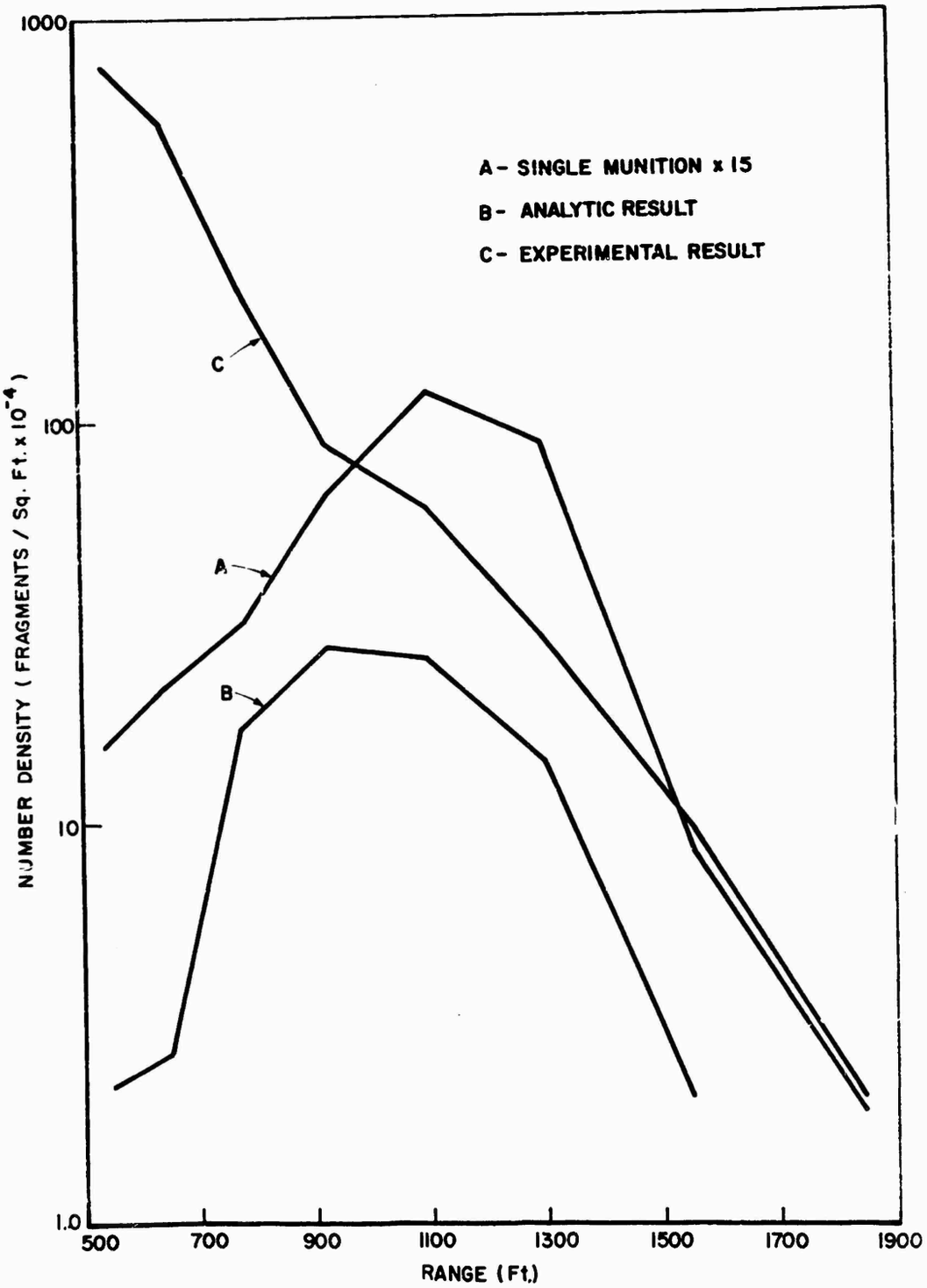

Figure 31 3x5 ANALYTIC-EXPERIMENTAL COMPARISONS FOR ALL FRAGMENTS

TABLE 13

RATIO OF NUMBER DENSITIES FOR SIX AND 15 BOMB TEST

Cell	Front Quarter	Nose	Back Quarter	Base	Side
1	4.4	1.93	2.95	2.68	4.54
2	3.1	3.14	2.1	4.75	1.96
3	4.1	2.06	3.24	3.2	1.59
4	1.9	12.7	3.82	12.1	1.06
5	7.6	4.9	2.01	8.1	1.88
6	1.2	55.	3.16	4.2	1.35
7	5.6	35.	3.80	4.12	1.75
8	1.91	130.	3.33	6.	1.0

7. CONCLUSIONS AND RECOMMENDATIONS

Based on the analytic and test results obtained in this study, one may conclude:

- The analytic model for predicting farfield terminal fragment effects confirms corresponding experimental results within an order of magnitude for comparable zones.
- From small-scale munition stack tests:
  - material enhancement zones have been seen to develop within discrete areas where one munition shades another
  - this enhancement has been seen to behave in a predictable manner at least for side-spray effects
  - celotex data indicate that material within enhancement areas can be divided into low and high energy fragments; low energy fragments resulting from down range collisions.

- o Current fragment input data for single munitions lacks sufficient resolution for heavier fragments to be useful as input to the analytic model without first modifying it.
- The China Lake full-size bomb tests confirm that enhancement takes place in the nose ogive and base selections of munitions as well as the sides.
- From the set of full-size shell tests conducted at Yuma:
  - indications are that fragment size may be strongly influenced by stack configurations, contact area of munitions within a stack, and the point of detonation
  - it is apparent that the acceptor stack has effectively blocked fragments from the donor stack
  - that effective design of stack configurations can minimize potential fragment hazards.

From these conclusions the following recommendations are made:

- In order to obtain an experimental verification of the mapping sections of the analytic model, a new set of full size, single munition experiments should be run to obtain farfield data for the M117 bomb. Such an experiment might include six repetitive explosions and just one recovery; averaging the results to obtain a statistically meaningful result.
- The fragment mass and number data, defined as a function of polar zone for a single bomb, should be investigated insofar as examining its sensitivity to the smoothing techniques which are presently applied to it.
- A whole new set of small-scale experiments should be conducted in order to be able to obtain amplification factors within the nose and base regions of a stack. Such a study might investigate the relationship of nose or base curvature to fragment enhancement.

This page is purposefully left blank.

This page is purposefully left blank.

APPENDIX

Fragment Distribution Data for M117 Bomb Stacks

- NWC Fragment Collection Cell Specification
- Six (6) Bomb Stack Data (3-high x 2-wide)
- Fifteen (15) Bomb Stack Data (3-high x 5-wide)
- Tests conducted at Naval Weapons Center, China Lake, California

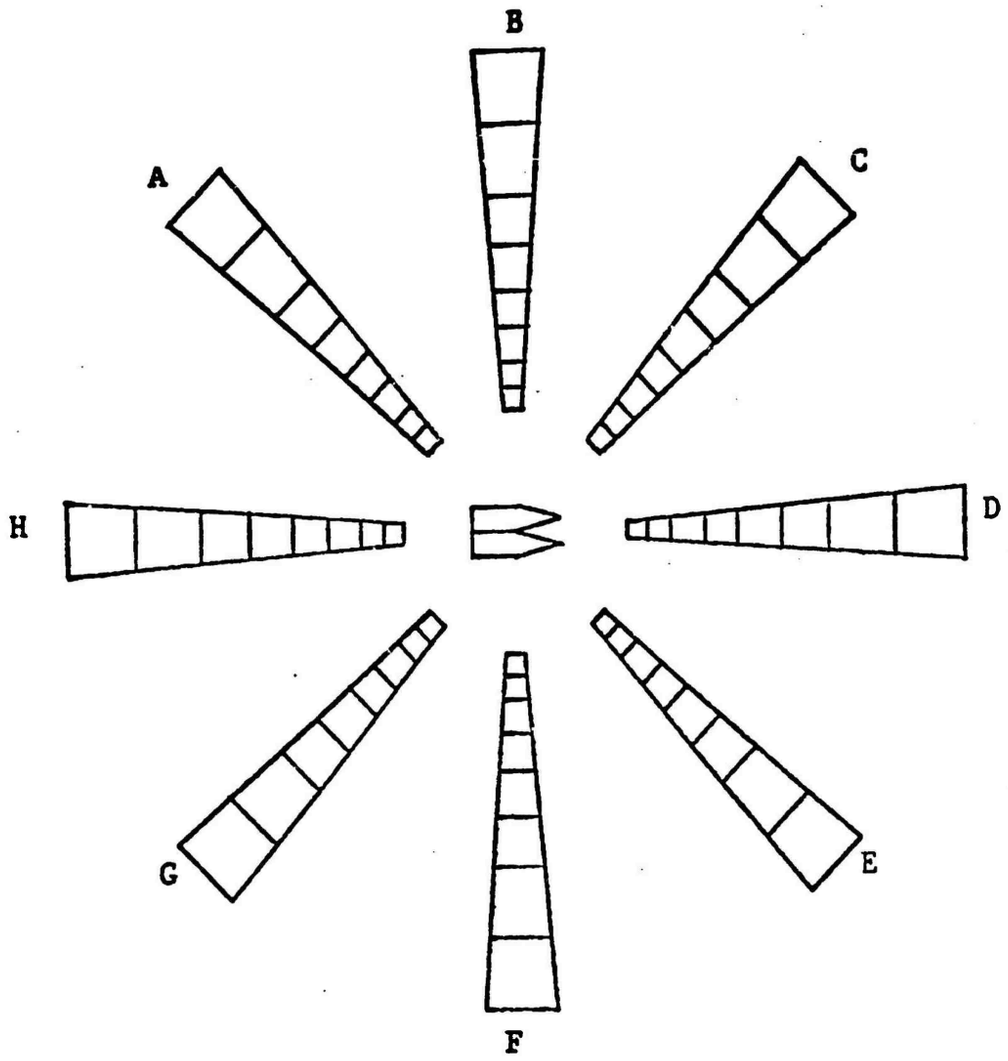

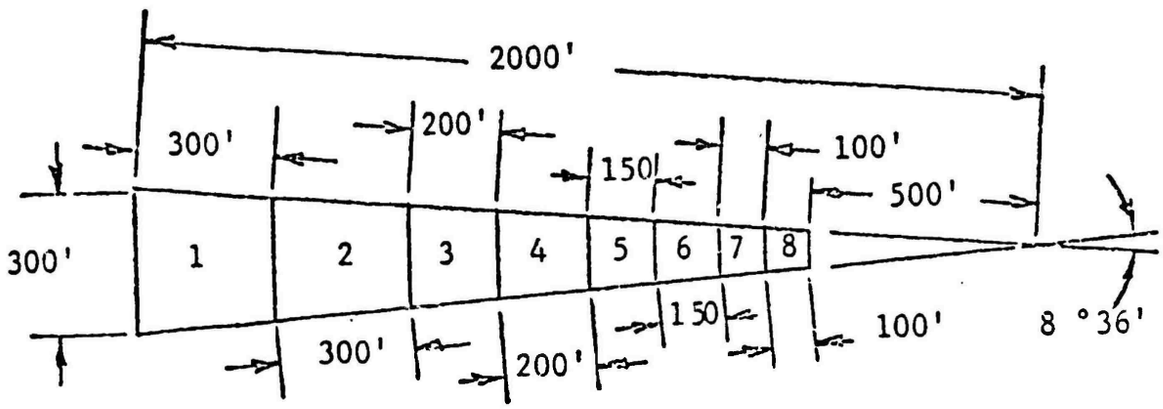

NWC FRAGMENT COLLECTION CELL SPECIFICATION

Fragment Distribution Data for M117 Bomb Stacks (6 Bombs)

MESH SIZE	AG-1		AG-2		AG-3		AG-4	
	Wt.(g)	No.	Wt.(g)	No.	Wt.(g)	No.	Wt.(g)	No.
1"	237	2	55.2	1	851	5	310	4
7/8"	--	--	67.8	1	--	--	138	2
3/4"	44.6	1	61.6	2	76.4	2	114	4
5/8"	--	--	19.6	1	78.5	3	172	7
1/2"	17.7	1	16.2	1	66.3	5	92.5	7
7/16"	10.4	1	--	--	--	--	52.1	6
3/8"	--	--	8.7	1	--	--	35.7	5
5/16"	--	--	--	--	--	--	7.3	2
1/4"	--	--	--	--	--	--	5.4	8
#4	2.1	1	--	--	--	--	3.8	4
#6	--	--	--	--	--	--	--	--
#8	--	--	--	--	--	--	--	--
< #8	--	--	--	--	--	--	5.5	--
	AG-5		AG-6		AG-7		AG-8	
1"	107	1	544	5	--	--	232	3
7/8"	58.6	1	45.8	1	133	2	174	2
3/4"	17.5	1	62.9	1	--	--	46.8	1
5/8"	107	5	23.3	2	163	6	18.7	1
1/2"	114	12	103	7	55.7	5	95.0	8
7/16"	73.2	11	32.2	5	58.4	6	24.8	3
3/8"	80.4	14	41.8	10	92.8	19	52.9	12
5/16"	31.1	10	37.8	12	62.1	24	42.3	16
1/4"	20.8	9	29.4	18	60.4	37	65.8	42
#4	3.6	3	9.2	9	49.2	61	58.8	76
#6	2.0	5	3.3	12	14.9	37	40.7	120
#8	--	--	1.2	4	2.8	16	7.7	43
< #8	2.4	--	1.3	--	10.5	--	12.0	--

Fragment Distribution Data for M117 Bomb Stacks (6 Bombs)

MESH SIZE	BF-1		BF-2		BF-3		BF-4	
	Wt. (g)	No.	Wt. (g)	No.	Wt. (g)	No.	Wt. (g)	No.
1"	871	6	1610	10	1035	13	1821	10
7/8"	182	2	657	7	816	12	656	9
3/4"	178	3	370	6	722	18	465	10
5/8"	201	7	315	9	512	17	690	22
1/2"	136	8	380	21	388	24	757	21
7/16"	17.2	3	97.0	9	133	13	245	30
3/8"	4.8	1	37.6	6	77.0	11	131	26
5/16"	5.7	1	5.2	2	25.4	8	70.3	18
1/4"	2.5	1	--	--	1.9	1	34.5	21
#4	--	--	1.7	2	5.4	4	10.4	12
#6	--	--	1.1	1	1.2	3	4.0	14
#8	--	--	--	--	--	--	0.8	9
< #8	--	--	7.0	--	22.4	--	63.9	--
	BF-5		BF-6		BF-7		BF-8	
1"	581	3	605	6	239	2	--	--
7/8"	289	6	178	3	184	3	134	2
3/4"	210	6	185	6	23.0	1	95.4	3
5/8"	585	24	199	9	67.5	4	84.5	4
1/2"	552	47	316	25	155	15	122	19
7/16"	387	50	149	22	147	21	76.6	10
3/8"	354	76	245	55	151	33	149	31
5/16"	215	67	289	92	175	68	158	59
1/4"	148	79	268	147	271	160	248	162
#4	51.4	59	123	135	209	250	309	429
#6	13.5	39	32.0	86	57.0	164	217	696
#8	2.0	11	3.7	27	--	--	51.5	359
< #8	132	--	120	--	--	--	27.5	--

Fragment Distribution Data for M117 Bomb Stacks (6 Bombs)

MASH SIZE	C-1		C-2		CE-3		C-4	
	Wt. (g)	No.	Wt. (g)	No.	Wt. (g)	No.	Wt. (g)	No.
1"	452	4	786	4	889	9	367	2
7/8"	90.9	2	192	2	361	6	34.7	1
3/4"	338	7	92.5	1	349	9	66.3	1
5/8"	118	3	88.7	4	463	19	69.3	4
1/2"	35.0	2	38.2	2	238	16	121	7
7/16"	9.7	1	--	--	68.3	7	42.7	5
3/8"	--	--	--	--	17.4	4	9.0	2
5/16"	--	--	--	--	18.2	4	11.6	4
1/4"	--	--	--	--	5.6	3	10.9	4
#4	--	--	--	--	2.2	3	--	--
#6	--	--	--	--	--	--	1.1	2
#8	--	--	--	--	--	--	--	--
< #8	--	--	--	--	17.2	--	--	--
	CE-5		CE-6		CE-7		CE-8	
1"	540	4	221	3	601	3	273	2
7/8"	126	2	267	3	141	2	--	--
3/4"	193	5	143	4	--	--	--	--
5/8"	91.0	4	75.2	3	110	6	124	6
1/2"	170	17	171	15	132	11	89.3	7
7/16"	168	19	114	16	56.0	8	37.6	6
3/8"	125	24	151	32	81.0	18	105	24
5/16"	73.3	20	127	37	69.2	27	55.3	19
1/4"	21.2	12	87.0	50	78.0	44	102	67
#4	11.2	12	47.7	51	54.7	62	123	156
#6	2.9	7	12.8	31	17.6	44	55.6	17[illegible]
#8	--	--	1.4	8	2.7	17	11.9	81
< #8	2.6	--	6.1	--	3.5	--	11.9	--

Fragment Distribution Data for M117 Bomb Stacks (6 Bombs)

MESH SIZE	D-1		D-2		D-3		D-4	
	Wt. (g)	No.	Wt. (g)	No.	Wt. (g)	No.	Wt. (g)	No.
1"	--	--	61.5	1	101	1	110	1
7/8"	51.5	1	166	3	--	--	126	1
3/4"	--	--	95.8	2	62.7	2	234	7
5/8"	27.5	1	83.8	3	--	--	324	15
1/2"	--	--	59.8	5	19.6	2	373	28
7/16"	--	--	23.3	3	21.2	2	76.8	7
3/8"	--	--	5.4	1	--	--	111.9	22
5/16"	--	--	--	--	3.9	1	56.4	17
1/4"	--	--	2.7	1	--	--	13.3	8
#4	--	--	--	--	--	--	10.0	10
#5	--	--	--	--	--	--	--	--
#8	--	--	--	--	--	--	--	--
< #8	--	--	--	--	--	--	--	--
	D-5		D-6		D-7		D-8	
1"	404	2	205	2	40.2	1	72.2	1
7/8"	--	--	40.2	1	--	--	--	--
3/4"	--	--	87.3	2	--	--	112	2
5/8"	51.9	2	59.2	4	53.2	3	19.3	1
1/2"	80.4	7	248	19	118	11	98.3	8
7/16"	26.5	4	166	25	51.4	8	18.0	2
3/8"	51.9	10	135	28	99.2	20	99.3	21
5/16"	20.1	5	98.2	29	66.4	22	54.2	19
1/4"	9.4	5	111	56	95.8	59	93.1	63
#4	2.6	2	55.0	58	67.9	79	119	155
#6	0.7	1	10.4	26	33.3	81	67.1	182
#8	--	--	2.3	9	3.9	23	10.7	73
< #8	--	--	9.1	--	9.7	--	9.6	--

Fragment Distribution Data for M117 Bomb Stacks (6 Bombs)

MESH SIZE	H-1		H-2		H-3		H-4	
	Wt.(g)	No.	Wt.(g)	No.	Wt.(g)	No.	Wt.(g)	No.
1"	1657	7	685	4	225	3	--	--
7/8"	291	2	228	4	127	2	53.1	1
3/4"	184	3	191	4	130	3	168	4
5/8"	122	1	366	7	135	5	141	5
1/2"	104	3	198	11	163	6	121	9
7/16"	--	--	80.9	3	22.0	3	156	20
3/8"	5.2	1	40.4	2	59.0	5	64.8	11
5/16"	--	--	3.9	1	32.1	9	47.2	15
1/4"	--	--	--	--	4.7	3	18.2	8
#4	1.0	1	--	--	2.2	1	3.4	5
#6	--	--	1.6	3	0.8	3	2.9	8
#8	--	--	--	--	0.5	1	0.8	5
< #8	3.2	--	4.3	--	3.8	--	3.6	--
	H-5		H-6		H-7		H-8	
1"	59.2	1	--	--	259	1	153	2
7/8"	158	4	40.3	1	35.1	1	98.5	2
3/4"	135	3	66.2	3	76.1	2	--	--
5/8"	52.5	2	197	8	20.7	1	--	--
1/2"	96.8	8	113	10	83.7	7	33.8	3
7/16"	23.7	4	90.3	11	72.7	10	40.8	5
3/8"	123	24	113	24	96.1	23	34.0	8
5/16"	60.5	19	88.7	30	72.3	28	54.9	21
1/4"	46.8	24	66.7	43	92.1	59	107	72
#4	13.2	15	50.4	58	76.2	102	133	185
#6	1.5	3	12.1	39	29.8	89	88.3	303
#8	1.4	7	1.8	12	6.5	45	26.4	203
< #8	175	--	64.4	--	25.4	--	51.1	--

Fragment Distribution Data for M117 Bomb Stacks (15 Bombs)

MESH SIZE	AG-1		AG-2		AG-3		AG-4	
	Wt. (g)	No.	Wt. (g)	No.	Wt. (g)	No.	Wt. (g)	No.
1"	291	2	715	5	541	4	542	4
7/8"	31.0	2	201	4	337	5	158	3
3/4"	86.8	2	230	6	441	11	251	7
5/8"	75.8	2	125	6	227	7	257	14
1/2"	75.3	5	50.3	3	218	15	171	16
7/16"	34.1	4	37.0	2	39.9	5	66.2	6
3/8"	5.0	1	13.6	3	14.2	3	92.3	16
5/16"	--	--	--	--	--	--	19.3	5
1/4"	--	--	--	--	7.4	2	12.2	7
#4	--	--	--	--	--	--	1.9	2
#6	--	--	--	--	--	--	1.8	3
#8	--	--	--	--	--	--	--	--
< #8	--	--	--	--	--	--	9.8	--
	AG-5		AG-6		AG-7		AG-8	
1"	469	4	558	6	412	4	241	3
7/8"	228	5	242	4	50.1	1	62.9	2
3/4"	388	10	133	4	184	5	188	5
5/8"	276	12	368	16	57.0	4	129	5
1/2"	341	28	252	22	337	26	279	24
7/16"	148	17	189	27	170	23	120	14
3/8"	133	23	216	45	213	45	169	36
5/16"	65.6	18	74.0	23	160	57	133	45
1/4"	35.6	16	91.1	45	131	73	190	116
#4	12.8	17	44.4	44	94.2	109	172	220
#6	3.5	12	8.6	24	28.2	74	93.4	274
#8	--	--	2.1	10	6.0	28	20.1	148
< #8	28.6	--	1.3	--	17.4	--	22.4	--

Fragment Distribution Data for M117 Bomb Stacks (15 Bombs)

MESH SIZE	CE-1		CE-2		CE-3		CE-4	
	Wt.(g)	No.	Wt.(g)	No.	Wt.(g)	No.	Wt.(g)	No.
1"	1061	5	1068	5	1682	12	1507	10
7/8"	207	4	185	4	216	4	255	4
3/4"	373	10	619	15	316	9	797	21
5/8"	364	12	543	18	472	17	728	31
1/2"	58.3	4	369	27	610	47	1072	90
7/16"	25.8	3	72.9	9	201	26	579	74
3/8"	12.2	2	57.0	11	116	24	391	80
5/16"	--	--	8.3	3	68.1	15	298	92
1/4"	--	--	3.8	2	18.5	9	128	73
#4	--	--	--	--	14.2	13	58.5	67
#6	--	--	--	--	--	--	12.3	36
#8	--	--	--	--	--	--	1.8	15
<#8	--	--	--	--	8.5	--	14.0	--
	CE-5		CE-6		CE-7		CE-8	
1"	1655	12	999	6	1690	10	561	5
7/8"	240	5	543	7	143	3	184	2
3/4"	307	7	208	6	150	4	122	4
5/8"	453	20	755	31	233	11	294	16
1/2"	684	52	832	64	475	40	488	39
7/16"	459	59	425	55	216	33	328	44
3/8"	473	105	442	95	331	77	271	60
5/16"	355	117	378	144	308	112	253	93
1/4"	260	153	486	304	387	242	354	221
#4	142	159	383	462	443	534	479	577
#6	28.0	93	166	489	318	935	424	1247
#8	6.7	46	33.6	240	91.3	652	207	1478
<#8	83.8	--	81.4	--	68.5	--	178	--

Fragment Distribution Data for M117 Bomb Stacks (15 Bombs)

MESH SIZE	D-1		D-2		D-3		D-4	
	Wt.(g)	No.	Wt.(g)	No.	Wt.(g)	No.	Wt.(g)	No.
1"	2713	22	1678	15	1318	9	973	9
7/8"	616	9	1248	23	672	11	334	6
3/4"	1959	47	1868	49	977	27	1071	31
5/8"	1143	43	2531	113	1452	69	1104	56
1/2"	1070	67	2454	179	1783	144	2195	188
7/16"	285	28	931	106	1021	128	1507	209
3/8"	123	21	655	110	906	166	1345	240
5/16"	26.5	6	296	87	456	138	1094	378
1/4"	21.5	9	91.3	49	270	131	789	493
#4	8.1	6	41.8	46	82.9	85	395	476
#6	--	--	11.1	28	15.0	38	103	303
#8	--	--	--	--	--	--	12.6	94
< #8	13.1	--	64.1	--	72.3	--	57.9	--
	D-5		D-6		D-7		D-8	
1"	514	6	1326	8	832	7	--	--
7/8"	55.4	1	166	4	226	4	127	2
3/4"	553	13	212	6	123	5	141	4
5/8"	568	29	702	35	271	12	142	6
1/2"	1070	91	650	56	236	19	165	15
7/16"	732	111	469	72	213	33	281	41
3/8"	1019	182	764	136	384	68	239	55
5/16"	981	338	799	275	370	128	274	96
1/4"	1147	718	1249	781	606	377	357	223
#4	924	1110	1657	1995	931	1121	644	776
#6	352	1035	1199	3530	1068	3140	817	2400
#8	50.5	360	380	2710	635	4540	602	4300
< #8	73.9	--	154	--	431	--	702	--

Fragment Distribution Data for M117 Bomb Stacks (15 Bombs)

MESH SIZE	H-1		H-2		H-3		H-4	
	Wt. (g)	No.	Wt. (g)	No.	Wt. (g)	No.	Wt. (g)	No.
1"	7440	37	3662	22	3199	8	835	10
7/8"	1659	18	1115	17	400	6	500	10
3/4"	629	10	1576	31	413	10	403	10
5/8"	724	17	903	25	730	23	586	24
1/2"	147	8	551	32	470	29	987	67
7/16"	154	5	267	17	349	24	317	34
3/8"	--	--	37.8	6	117	20	244	43
5/16"	--	--	13.4	3	29.2	8	76.0	23
1/4"	--	--	--	--	10.9	6	33.7	18
#4	--	--	--	--	5.4	3	6.4	6
#6	--	--	--	--	2.5	6	2.3	6
#8	--	--	--	--	2.2	18	--	--
< #8	6.2	--	11.6	--	10.2	--	17.2	--
	H-5		H-6		H-7		H-8	
1"	339	5	1497	10	554	3	610	4
7/8"	218	4	204	5	102	2	64.0	2
3/4"	170	6	292	10	123	3	25.8	1
5/8"	524	26	317	16	305	18	28.6	1
1/2"	779	64	672	61	327	31	298	24
7/16"	554	64	473	68	237	33	150	22
3/8"	437	85	684	138	345	78	260	59
5/16"	234	65	422	138	300	107	241	90
1/4"	85.9	39	326	169	393	237	413	272
#4	25.4	27	141	138	274	318	505	649
#6	5.7	13	19.9	52	67.6	192	277	815
#8	1.3	6	2.1	12	11.8	69	81.0	578
< #8	21.4	--	39.7	--	39.5	--	62.2	--